# Stable and radiogenic isotopic signatures of mineralized Devonian carbonate rocks of the northern Rocky Mountains and the Western Canada Sedimentary Basin

S. Paradis[1], W.A. Turner[2], M. Coniglio[3], N. Wilson[4] and J.L. Nelson[5]

Paradis, S., Turner, W.A., Coniglio, M., Wilson, N., and Nelson, J.L., 2006: Stable and radiogenic isotopic signatures of mineralized Devonian carbonate rocks of the northern Rocky Mountains and the Western Canada Sedimentary Basin; *in* Potential for Carbonate-hosted Lead-zinc Mississippi Valley-type Mineralization in Northern Alberta and Southern Northwest Territories: Geoscience Contributions, Targeted Geoscience Initiative, (ed.) P.K. Hannigan; Geological Survey of Canada, Bulletin 591, p. 75–103.

**Abstract:** Mineralized and non-mineralized coarse-crystalline dolomite (CCD) and saddle dolomite (SD) in Devonian carbonate rocks of the northern Rocky Mountains and the Western Canada Sedimentary Basin are compared in terms of fluid inclusion microthermometry and stable and radiogenic isotopic characterization. Samples from the Western Canada Sedimentary Basin are divided into four areas: eastern Presqu'ile barrier, western Presqu'ile barrier, McDonald–Hay River Fault system, and the Peace River Arch.

Isotopic trends point to easterly formation-fluid flow paths from the Rocky Mountains to the western continental platform, and a key role for the northeast-trending structures in the circulation and focusing of hydrothermal and mineralizing fluids.

Two distinct lead isotopic populations exist in sulphides from the carbonate-hosted Zn-Pb occurrences of the northern Canadian Rocky Mountains, Mackenzie Mountains, and Western Canada Sedimentary Basin, suggesting that two separate fluid sources/pathways existed in the Western Canada Sedimentary Basin.

**Résumé :** Nous avons comparé la dolomite en gros cristaux et la dolomite en forme de selle, minéralisées et non minéralisées, contenues dans des roches carbonatées dévoniennes des Rocheuses septentrionales et du Bassin sédimentaire de l'Ouest du Canada, par microthermométrie des inclusions fluides et par caractérisation des isotopes stables et radiogéniques. Les échantillons en provenance du Bassin sédimentaire de l'Ouest du Canada ont été divisés selon quatre zones : la partie est de la barrière de Presqu'ile, la partie ouest de la barrière de Presqu'ile, le réseau de failles de McDonald-Hay River et l'arche de Peace River.

La distribution des isotopes donne a penser que les trajets d'écoulement des fluides de formation étaient vers l'est, soit depuis les Rocheuses vers la plate-forme continentale occidentale, et que les structures orientées nord-est ont joué un rôle déterminant pour la circulation et la convergence des fluides hydrothermaux et minéralisateurs.

Il existe deux populations distinctes d'isotopes du plomb dans des sulfures provenant d'indices de zinc-plomb encaissés dans des roches carbonatées dans le nord des Rocheuses canadiennes, dans les monts Mackenzie et dans le Bassin sédimentaire de l'Ouest du Canada, ce qui porte à croire que deux sources ou voies distinctes pour les fluides existaient dans le Bassin sédimentaire de l'Ouest du Canada.

[1] Geological Survey of Canada, 9860 West Saanich Road, Sidney, BC, V8L 4B2, suparadi@NRCan.gc.ca
[2] C.S. Lord Northern Geoscience Centre, P.O. Box 1500, Yellowknife, NWT, X1A 2R3, allan_turner@gov.nt.ca; cslord_centre@gov.nt.ca*
[3] Department of Earth Sciences, University of Waterloo, 200 University Avenue West, Waterloo, ON, N2L 3G1, coniglio@uwaterloo.ca
[4] Geological Survey of Canada, 3303 33 Street N.W., Calgary, Alberta, T2L 2A7, nwilson@NRCan.gc.ca**
[5] British Columbia Geological Survey Branch, Box 9320 Stn. Prov. Govt., Victoria, BC, V8W 9N3, joanne.nelson@gems1.gov.bc.ca
* Now at Elemental Geological Services Ltd., 9143-71 Ave., Edmonton, Alberta T6E 0V9, allan_turner@telus.net
** Now at Talisman Energy Inc., Suite 3400, 888-3rd St. S.W., Calgary, Alberta, T2P 5C5, nwilson@talisman-energy.com

# INTRODUCTION

Paleozoic sedimentary rocks of the Canadian Rocky Mountains and the Western Canada Sedimentary Basin (WCSB) host a number of stratabound and stratiform Zn-Pb deposits (Fig. 1). In the northern Rocky Mountains, the deposits form a series of belts including the Devonian-Mississippian (and older) sedimentary exhalative (SEDEX) deposits of the Kechika Trough and Selwyn Basin, and the Mississippi Valley-type (MVT) deposits in Silurian–Devonian platform dolomite of the outcropping carbonate front (Thompson, 1989). Below the upper Paleozoic–Mesozoic cover, the carbonate front extends eastward as the Presqu'ile barrier, which hosts the Pine Point MVT Zn-Pb deposits in the Northwest Territories (NWT). Scattered galena and sphalerite are associated with coarse-crystalline dolomite (CCD) and saddle dolomite (SD) in Devonian carbonate of the WCSB both within and external to the Presqu'ile barrier, and in the Manetoe facies in the southern Mackenzie Mountains.

The development of CCD and SD is widespread in subsurface- and outcrop-carbonate rocks of the Rocky and Mackenzie Mountains and the WCSB, whereas Zn-Pb sulphide mineralization is sporadic. The distribution of Zn and Pb sulphide deposits in these regions is the product of regional or subcontinental-scale paleohydrological processes that have been traditionally explained by two models: 1) fluid circulation related to the Late Devonian–Early Mississippian Antler orogeny (Nesbitt and Muehlenbachs, 1994; Amthor et al., 1993; Mountjoy et al., 1999), and 2) fluid circulation related to the Cretaceous–Tertiary Laramide orogeny (Garven, 1985; Qing and Mountjoy, 1992, 1994, 1995; Adams et al., 2000). A third model was recently introduced by Paradis and Nelson (2000) and Nelson et al. (2002), involving deep convective circulation of hydrothermal fluids during Devonian–Mississippian time on the western margin of North America, in relation to regional extension caused by slab rollback, and generation of back-arc and intra-arc spreading and exhalative activity. They suggested that MVT carbonate-hosted Zn-Pb deposits and hydrothermal dolomite in the Rocky Mountains and the WCSB are related to these events, with fluids driven along reactivated back-arc faults and permeable strata.

This contribution builds on the previous work of Paradis and Nelson (2000) and Nelson et al. (2002),who suggested that MVT carbonate-hosted Zn-Pb mineralization and hydrothermal dolomite in the northern Rocky Mountains and the WCSB, both within and external to the Presqu'ile barrier, are Devonian–Mississippian in age and genetically related. We first address the question of whether the mineralized and nonmineralized CCD and SD of these regions have the same isotopic signatures, and verify the existence of spatial isotopic trends. We then discuss the results in terms of fluid flow and mineralizing systems.

# METHODOLOGY

## Sampling and classification

Mineralized samples were collected for isotopic and fluid inclusion (also see Turner, 2006) analyses from drill-cored intervals of subsurface Devonian carbonate rocks of the Manetoe facies in the Mackenzie Mountains, the WCSB, both within and external to the Presqu'ile barrier, and from outcrops in the Rocky Mountains (Fig. 1). Along the eastern Presqu'ile barrier, samples were collected west of the Pine Point deposits, that is, within the Great Slave Reef (Fig. 2, 3), Hay West (Fig. 2, 4), Windy Point (Fig. 2), and Qito (Fig. 2) mineral properties. Samples previously collected (Nelson et al., 2002) from the western Presqu'ile barrier and the Robb Lake deposit in the Rocky Mountains were included for comparison.

We refer to the eastern Presqu'ile barrier as encompassing the Pine Point, Great Slave Reef, Hay West, Windy Point, and Qito mineral properties (see location on Fig. 1), and situated between the longitudes of 114 and 117°W. The western Presqu'ile barrier is situated west of 117°W and its western boundary is defined by the Cordilleran deformation front (see location on Fig. 1).

Examination of the samples was done by petrographic microscopy and cathodoluminescence microscopy (CL) using a Technosyn cold cathodoluminescence unit at a 15–17 kV beam voltage and 0.7–0.8 mA beam current. Carbonate samples were classified by mineralogy and crystal size following Qing (1991), Qing and Mountjoy (1994) and Turner (2006) terminology. The dolomite samples were divided into fine-crystalline dolomite (FCD), medium-crystalline dolomite (MCD), coarse-crystalline dolomite (CCD), and saddle dolomite (SD). The CCD and SD are the focus of this study. They show close spatial and temporal relationships with MVT Zn–Pb mineralization in the Rocky Mountains and the WCSB, although the CCD and SD are more widespread in the subsurface and outcrop than sulphide mineralization (Machel and Mountjoy, 1986; Leach and Sangster, 1993). The CCD and SD are also known as the "Presqu'ile dolomite" (Norris, 1965; Skall, 1975; Kyle 1981; Krebs and Macqueen, 1984; Rhodes et al., 1984; Qing, 1991; Qing and Mountjoy, 1994) or hydrothermal dolomite (Qing, 1991; Qing and Mountjoy, 1994; Davies, 1997; Morrow, 1998; Adams et al., 2000; Al-Aasm, 2003).

## Fluid inclusion microthermometry

Fluid inclusion microthermometric analyses were performed on doubly polished thin sections using a Linkam THMSG 600 heating and freezing stage attached to a CI 93 programmer and LNP cooling pump at the University of Alberta and Geological Survey of Canada. Calibration of the analytical equipment was carried out using synthetic fluid inclusion standards manufactured by Syn Flinc. Accuracy was determined to within ±0.2°C for freezing runs and ±2°C

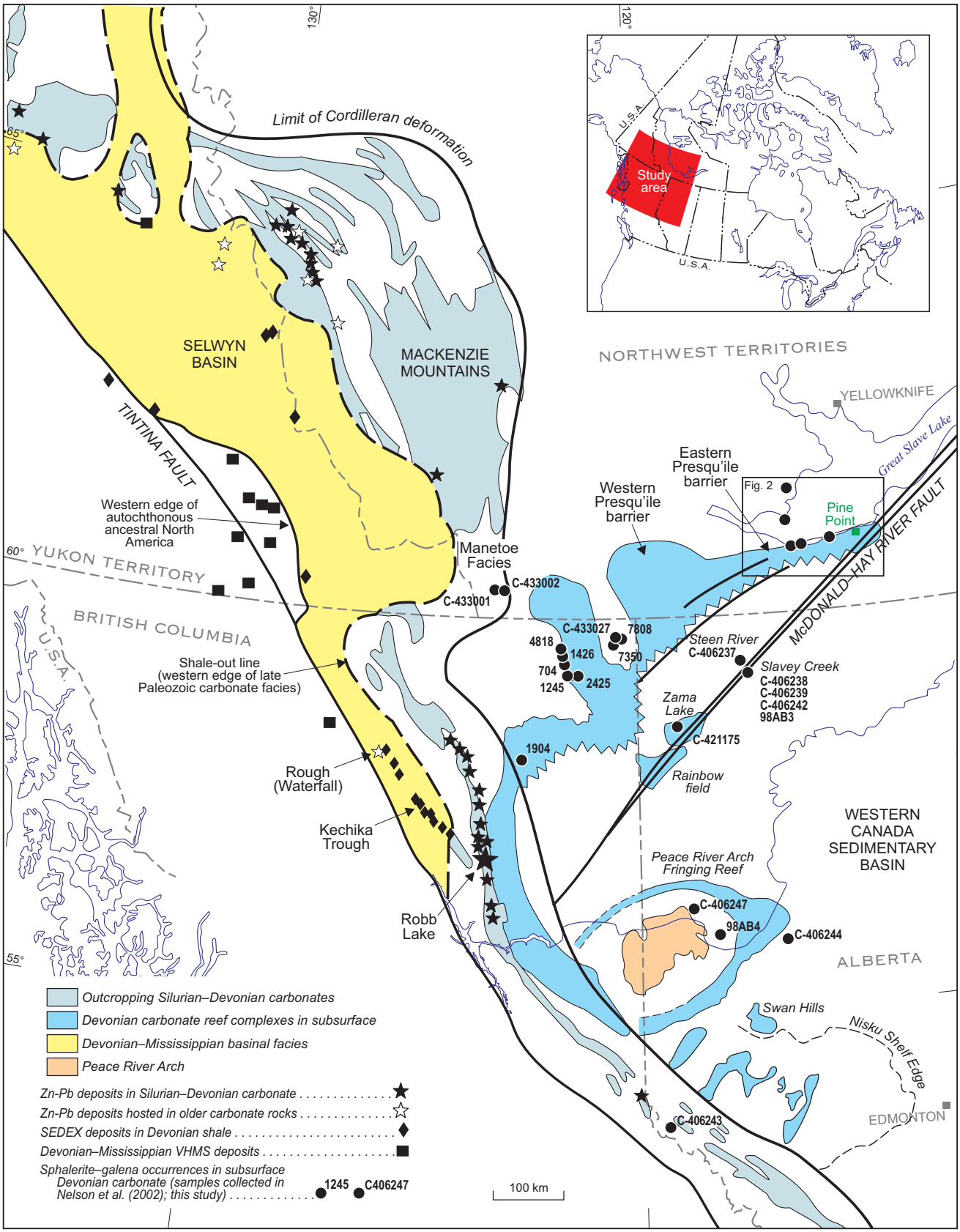


**Figure 1.** Location of western Canadian carbonate-hosted Zn-Pb deposits, subsurface carbonate-hosted sphalerite and galena occurrences, and sedimentary exhalative (SEDEX) deposits, and their stratigraphic, structural, and tectonic setting within Paleozoic rocks in the Western Canada Sedimentary Basin and northern Canadian Rocky Mountains. Also shown is the location of samples examined in this study and in Nelson et al. (2002). Rectangle including the Pine Point deposits outlines the location of Figure 2. Diagram is *compiled from* Morrow et al. (1990), Olson et al. (1994), and Mossop and Shetsen (1994).

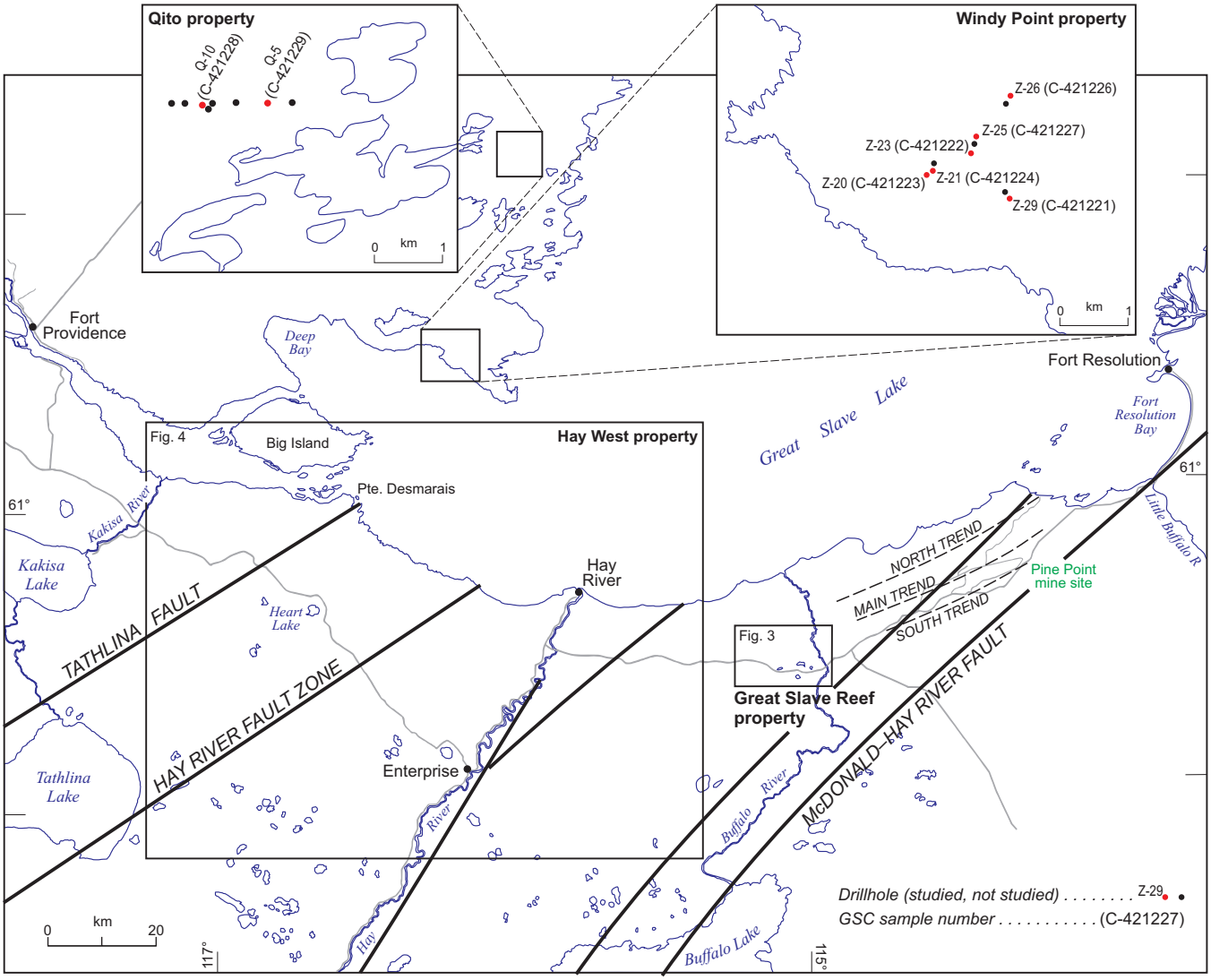


**Figure 2.** Location map of the mineral properties along the eastern Presqu'ile barrier. Outlined areas indicate the locations of the mineral properties. Figure is *modified from* Turner (2006). Major faults are shown as bold lines (locations *after* Morrow et al., 2006).

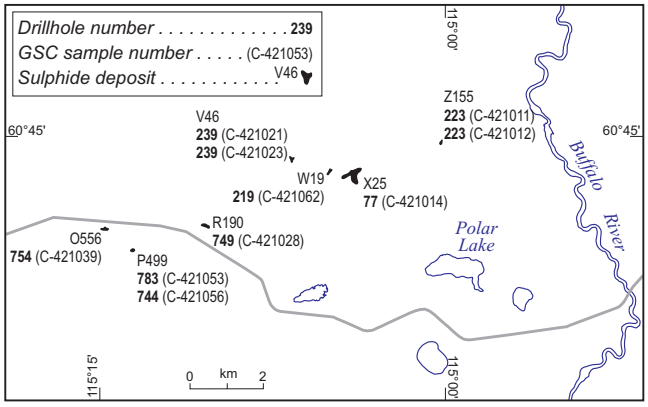


**Figure 3.** Orebodies within the Great Slave Reef property (located in Fig. 2). Figure is *modified from* Turner (2006).

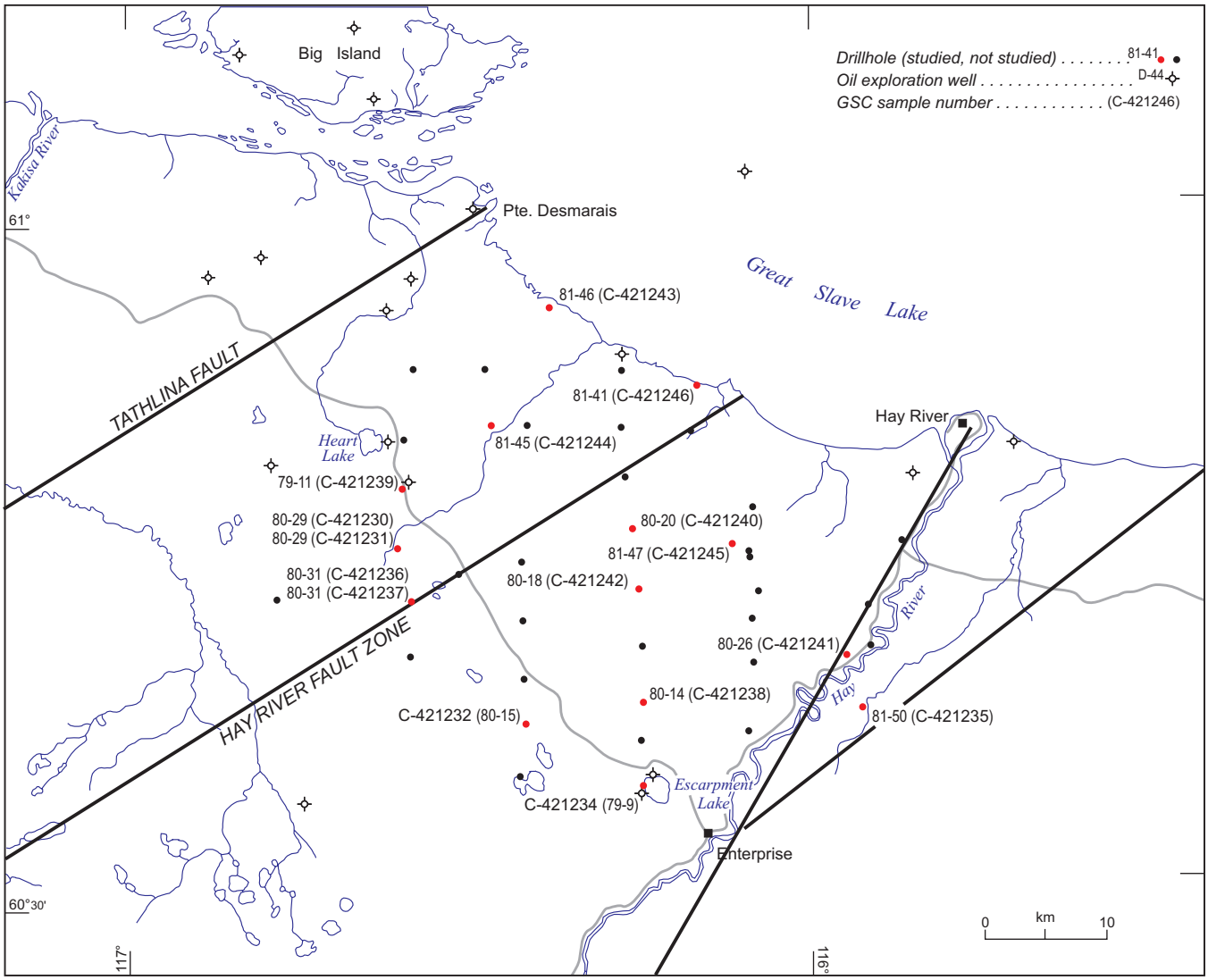


**Figure 4.** Drillhole locations on the Hay West property from which stable and radiogenic isotope analyses were carried out. Figure is *modified from* Turner (2006). Major faults are shown as bold lines (locations *after* Morrow et al., 2006).

for heating runs up to 300°C. Salinities were calculated from final ice melting temperatures using the equation of Bodnar and Vityk (1994) and are reported as wt.% NaCl equiv. Compositions of saline, $CaCl_2$-rich fluids were estimated graphically using the NaCl-$CaCl_2$-$H_2O$ ternary phase diagrams of Oakes et al. (1990, 1992). Fluid inclusion assemblages (FIAs) were made on primary two-phase aqueous (liquid+vapour) inclusions.

## Carbon, oxygen, and strontium isotopes

Carbon and oxygen isotope analyses were completed on 50 samples of CCD and SD at the Isotope Science Laboratory in the Department of Physics and Astronomy at the University of Calgary. Samples were drilled and hand picked from rock slabs using 100 µm-diameter drill bits. Carbon and oxygen isotopic compositions were determined on 10 to 20 mg of powdered sample by analysis of $CO_2$ generated by reaction with 3 ml of 100% phosphoric acid (McCrea, 1950). Digestion was done at 25°C. All dolomite samples were subjected to a two-stage procedure whereby $CO_2$ from any possible calcite was produced after the first 3 to 5 hours of reaction and then frozen in a breakseal vessel. After 72 hours, the remaining $CO_2$ from dolomite was sealed in a second breakseal vessel. Only the results from the 2nd stage of the analysis are reported for dolomite. The evolved $CO_2$ gas was analyzed for $^{18}O/^{16}O$ and $^{13}C/^{12}C$ using a VG 903 dual inlet isotope mass spectrometer. Results are reported in conventional per mil notation (‰) relative to PDB (Peedee belemnite), and corrected for $^{17}O$ as described in Craig (1957). No correction for acid fractionation was made for dolomite (Friedman and O'Neil, 1977). Precision, based on replication of international and internal standards, is ±0.2 ‰ and ±0.3 ‰ for C and O, respectively.

Strontium analyses were carried out on 37 samples of dolomite at the Radiogenic Isotope Facility at the University of Alberta. The same samples were also analyzed for O and C isotopes (except for C-421175). One hundred mg of dolomite sample powders were weighed out in Teflon screw-cap vials and dissolved in dilute, cold (approx. 0.75N) HCl. This was done to minimize any Sr release from potential contaminant silicate phases, such as clays. After centrifugation, Sr was separated by conventional cation exchange chromatography, and the isotopic composition determined by Thermal Ionization Mass Spectrometry (TIMS). Isotope ratios were normalized to $^{86}Sr/^{88}Sr = 0.11940$ to correct for fractionation and are presented relative to a value of 0.710245 for the NIST Standard Reference Material SRM987 Sr isotope standard. Uncertainty in $^{87}Sr/^{86}Sr$ is expressed as ±2 sigma of the mean, equivalent to two standard errors (2SE).

### Lead isotopes

Lead isotopic analyses were performed on clean cubes of galena and grains of sphalerite at the Radiogenic Isotope Facility of the University of Alberta. Those reported in Nelson et al. (2002) were done at the University of British Columbia Pacific Centre for Isotopic and Geochemical Research. Galena samples were dissolved in dilute (approx. 2N) HCl at approximately 50°C, and subsequently treated with 4N HCl to remove Fe and Zn impurities. Sphalerite samples were dissolved in hot 6N HCl and converted to bromides with the addition of HBr. Pb was separated by conventional anion exchange chromatography. The isotopic composition of Pb was determined by Thermal Ionization Mass Spectrometry (TIMS). All data were corrected for instrumental fractionation empirically using the Pb isotope standard SRM981 run under identical experimental conditions. At 1sigma error level, long-term reproducibility of the measured isotopic ratios is 0.024% for $^{206}Pb/^{204}Pb$, 0.036% for $^{207}Pb/^{204}Pb$, and 0.044% for $^{208}Pb/^{204}Pb$.

## GEOLOGICAL SETTING

Figure 1 illustrates the Devonian–Mississippian tectonic and metallogenic framework of the northern Canadian Cordillera and the WCSB, and the location of the samples analyzed in this study. The stratigraphy of the Paleozoic rocks of the WCSB to the south and west of Great Slave Lake has been documented in detail by several authors (see below) and therefore only a brief review is provided here. The Paleozoic stratigraphy of the northern Canadian Cordillera is discussed in Thompson (1989) and Ferri et al. (1999).

Throughout most of the WCSB, Paleozoic strata are deeply buried below the Mesozoic and Tertiary cover, and are only known from petroleum wells and seismic surveys. The WCSB consists of relatively undisturbed Middle Proterozoic to Lower Tertiary sedimentary successions that thicken to the west toward the Cordillera and thin to the east to an erosional edge against the Precambrian rocks of the Canadian Shield (Douglas et al., 1970). To the west, within the Cordilleran-deformed belt, Silurian to Middle Devonian shelf strata are exposed in the northern Rocky Mountains of British Columbia (BC) and in the Mackenzie Mountains of eastern Yukon and western NWT. In the northern Rocky Mountains, these strata host a series of MVT Zn-Pb deposits, most notably the Robb Lake deposit (Fig. 1). The Devonian carbonate front in the Rocky Mountains extends eastward to become the Presqu'ile barrier in the WCSB, a Middle Devonian carbonate reef complex, which hosts the Pine Point MVT Zn-Pb deposits (Fig. 1). The Presqu'ile barrier dips shallowly to the west, extends to the southwest for approximately 400 km, and varies between 20 and 90 km in width (Qing and Mountjoy, 1994). During the Middle Devonian, the barrier formed a bathymetric high, which restricted seawater movement, allowing shale and carbonate deposits of the Mackenzie Basin to develop north of the barrier and evaporite and carbonate to precipitate in the Elk Point Basin to the south. The Presqu'ile barrier, which consists of various carbonate reef facies of the Pine Point and Sulphur Point formations, developed on the shallow-water platform dolostone of the Keg River Formation. Shale, argillaceous limestone/dolostone, and anhydrite of the Watt Mountain and Slave Point formations overlie the barrier and its equivalents. A regional unconformity, the sub-Watt Mountain, separates the Pine Point and Sulphur Point formations of the barrier from the overlying Watt Mountain and Slave Point formations.

Zinc-lead mineralization at the Pine Point mine site (Fig. 2) is confined to three large dissolution channelways (North, Main, and South trends) that formed in specific carbonate facies along the strike of the Presqu'ile barrier (Kyle, 1981; Rhodes et al., 1984). Westmin Resources Limited extrapolated the Main Trend to the west of Buffalo River and discovered seven additional orebodies within the Great Slave Reef property (Randall et al., 1986; Turner et al., 2002; Fig. 2, 3), bringing the total number of known sulphide deposits in the Pine Point district to 100. In the late 1970s and early 1980s, Pine Point Mines Limited carried out exploration to the west of Hay River (Hay West property; Fig. 2, 4) and to the northwest of Great Slave Lake (Windy Point and Qito properties; Fig. 2). Zones of CCD and SD were identified within the Hay West, Windy Point, and Qito properties, but only sporadic pockets of sulphide mineralization were intersected in drill cores.

The Pine Point MVT Zn-Pb deposits are situated along the north side of the McDonald–Hay River Fault (Fig. 1), which forms the buried southwestern extension of the Great Slave Shear Zone, a dextral transcurrent fault within the crystalline Precambrian basement. The fault can be traced under the WCSB to the edge of the Cordilleran-deformed belt by its strong expression on aeromagnetic maps (Hoffman, 1987; Ross et al., 1991). South of the McDonald–Hay River Fault, the Peace River Arch (Fig. 1) was a stable, major east-northeast-trending basement structure prior to the deposition of the Middle Devonian carbonate in the WCSB.

In the northern Rocky Mountains, the Kechika Trough is an intracontinental basin situated immediately west of the exposed carbonate MVT belt. It is characterized by Lower Cambrian to Mississippian deep-water sediment (McClay et al., 1989) that hosts Late Devonian SEDEX Zn-Pb-barite deposits (Fig. 1; Paradis et al., 1998). The Selwyn Basin in the Yukon is analogous to the Kechika Trough, also containing SEDEX deposits of Cambrian through to Early Mississippian age. West of Kechika Trough and Selwyn Basin lie the Cassiar and McEvoy platforms, which are composed of shelf and shelf-slope sedimentary facies that were deposited oceanward of ancestral North America. The westernmost tectonic elements of the Canadian Cordillera are the allochthonous and para-autochthonous pericratonic terranes, which made up the active margin of North America in mid to late Paleozoic time. The pericratonic terranes contain widespread Devonian–Mississippian arc and arc-rift volcanic and plutonic suites with accompanying volcanic-hosted massive sulphide (VHMS) deposits (Nelson et al., 2002). Overall, these features depict the active continental margin of ancestral North America during Devonian–Mississippian time.

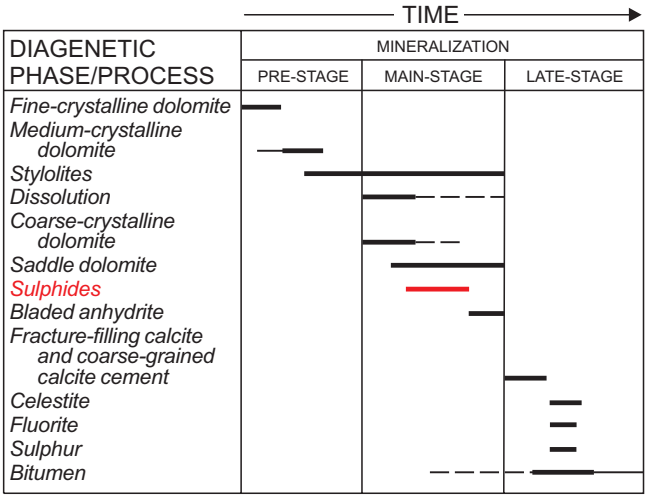


**Figure 5.** Generalized paragenetic sequence of the Presqu'ile barrier samples examined in this study. *Modified from* Kyle (1981), Krebs and Macqueen (1984), and Qing and Mountjoy (1994).

## PETROGRAPHY AND PARAGENESIS

The petrographic characteristics and paragenesis of the various diagenetic features and sulphide deposits in the Presqu'ile barrier and the WCSB have been documented by many authors including Fritz and Jackson (1972), Skall (1975), Kyle (1977, 1981), Krebs and Macqueen (1984), Rhodes et al. (1984), Qing (1991), Qing and Mountjoy (1994), and Coniglio et al. (2006). Four types of dolomite have been recognized in our study. From oldest to youngest they are fine-crystalline dolomite (FCD), medium-crystalline dolomite (MCD), coarse-crystalline dolomite (CCD), and saddle dolomite (SD). This textural and crystal size classification follows that of Qing (1991), Qing and Mountjoy (1994), and Turner (2006). A generalized paragenetic sequence is summarized in Figure 5. It is divided into pre-, main-, and late-stage mineralization, with the main-stage corresponding to precipitation of sulphide minerals.

The pre-mineralization stage consists of widespread dolomitization of limestone to a FCD. This is followed by formation of the MCD, and then the CCD and SD, which are the typical dolomites associated with sulphide minerals. The CCD and SD are generally referred to as the "Presqu'ile dolomite" (e.g. Norris, 1965; Skall, 1975; Kyle 1981; Krebs and Macqueen, 1984; Rhodes et al., 1984; Qing, 1991; Qing and Mountjoy, 1994) or hydrothermal dolomite (e.g. Qing, 1991; Qing and Mountjoy, 1994; Davies, 1997; Morrow, 1998; Adams et al., 2000; Al-Aasm, 2003). These dolomite types are mostly fabric destructive and precipitated slightly before or contemporaneously with sulphide minerals. Krebs and Macqueen (1984) observed that SD predates, is synchronous with, or postdates sulphide mineralization. Qing and Mountjoy (1994) noted that CCD and SD are contemporaneous with sulphide mineralization in the Presqu'ile barrier.

In our study, CCD consists of subhedral to anhedral white to light brown dolomite crystals ranging from approximately 500 µm to 2 mm. Under CL, CCD has dull to weak red luminescence with bright red specks. It occurs as replacement of the FCD and MCD, and as fracture- and vug-filling cement. SD is characterized by large white crystals (approx. 500 µm to 5 mm) that have curved faces and undulatory extinction. SD displays turbid inclusion-rich crystal cores with clear, inclusion-poor rims. Under CL, inclusion-rich crystal cores have a "blotchy" luminescence that appears as a mixture of irregular domains of bright red and dull or weak red luminescence. SD occurs primarily as fracture-, vug-, and breccia-filling cement.

Sulphide minerals associated with the main-mineralization stage at the mineral properties within the eastern Presqu'ile barrier consist of sphalerite, galena, marcasite, and pyrite. Sulphide precipitation generally begins with pyrite and marcasite and ends with sphalerite and galena. Sulphide textures are mostly related to open-space filling of breccias, fractures, and vugs. The sulphides are disseminated, massive, and banded. Disseminated sulphides occur as fine to coarse crystals of sphalerite and galena overlain by, or intergrown with CCD and SD. Coarse sphalerite crystals occasionally coat the tops of fragments or line the bottoms of cavities forming a texture known as "snow on roof" (Leach and Sangster, 1993; Sangster, 1995). Sphalerite also forms massive aggregates of coarse-grained colloform and botryoidal crystals and laminae of fine-grained crystals. Galena occurs as medium- to coarse-grained euhedral crystals and aggregates embedded with sphalerite. Skeletal galena inclusions in sphalerite are occasionally observed.

Following the main mineralization stage, further fracturing, dissolution, and saddle dolomite cement precipitation occurred. The latest mineral phases to precipitate are bladed anhydrite, coarse-crystalline calcite cement, celestite, fluorite, native sulphur, and bitumen (e.g. Kyle, 1981).

# FLUID INCLUSIONS

Fluid inclusion studies have previously been completed on SD from the eastern and western Presqu'ile barrier (i.e. Roedder, 1968; Qing, 1991; Qing and Mountjoy, 1994; Turner, 2006), and on sphalerite from the Great Slave Reef, Windy Point, and Pine Point properties (i.e. Roedder, 1968; Kyle, 1981; Turner, 2006). Results of the fluid inclusion microthermometry done on a few dolomite and sphalerite samples from the Great Slave Reef property and the Slavey Creek area along the McDonald-Hay River Fault are reported here.

Fluid inclusions in sphalerite and SD are typically ≤10 µm in size and are aqueous two-phase inclusions at room temperature (Fig. 6a, b). In the Great Slave Reef property (e.g. samples C-421014 and C-421039; Fig. 6a, c), sphalerite contains primary inclusions in the grain cores that have $Th_L$ (homogenization temperature to liquid phase) values of 70° to 95°C, and SD has inclusions that have $Th_L$ values of 75 to 145°C (17/20 analyses = 90–125°C). Ice melting temperatures ($Tm_{ice}$) indicate high salinity (29–34 wt.% NaCl equiv.) NaCl-$CaCl_2$ fluids. $Th_L$ values of 105 to 125°C were recorded in sphalerite from the Slavey Creek area (e.g. sample C-406241; Fig. 6b), but $Tm_{ice}$ was not collected.

# OXYGEN, CARBON, AND STRONTIUM ISOTOPES

$\delta^{18}O$, $\delta^{13}C$, and $^{87}Sr/^{86}Sr$ analyses of mineralized CCD and SD from the northern Rocky Mountains, Mackenzie Mountains, and WCSB are listed in Table 1. Ranges and averages of nonmineralized and mineralized dolomite samples are listed in Tables 2 and 3, respectively. The data are presented, and compared with published fields of nonmineralized CCD and SD from throughout the WCSB, on standard cross plots of $^{13}C$ vs. $\delta^{18}O$, $^{87}Sr/^{86}Sr$ vs. $\delta^{18}O$, and $^{87}Sr/^{86}Sr$ vs. $\delta^{13}C$ in Figure 7.

## Nonmineralized dolomite

$\delta^{18}O$ values of the nonmineralized CCD and SD from the eastern Presqu'ile barrier range from -13.0 to -7.0‰ (Fig. 7a and Table 2) and decrease slightly in the western Presqu'ile barrier with values ranging from -16.0 to -8.7‰. $\delta^{13}C$ values of the nonmineralized CCD and SD range from -2.2 to +2.5‰ for the eastern Presqu'ile barrier and from -3.8 to +2.7 ‰ for the western Presqu'ile barrier (Fig. 7a and Table 2). The $\delta^{13}C$ values don't show any spatial or stratigraphic trends (Qing, 1991; Qing and Mountjoy, 1994). $^{87}Sr/^{86}Sr$ ratios of the nonmineralized CCD and SD from the eastern Presqu'ile barrier range from 0.7081 to 0.7088, and increase to values ranging from 0.7085 to 0.7121 in the western Presqu'ile barrier (Table 2). All these dolomite samples (except sample NWT072; Mountjoy et al., 1992) plot below the Sr isotope ratio of 0.7120 (Fig. 7), which defines the regional background value of the "Maximum Sr Isotope Ratio of Basinal Shale" (MASIRBAS; Machel and Cavell, 1999) in the Cordillera.

SD from the Sulphur Point and Keg River formations of the Rainbow petroleum field in northern Alberta has narrow ranges of $\delta^{18}O$ and $\delta^{13}C$ values (Fig. 7a and Table 2). $\delta^{18}O$ values range from -13.7 to -10.7‰ for the Sulphur Point Formation and -10.65 to -7.8‰ for the Keg River Formation. $\delta^{13}C$ values range from -1.4 to +0.2‰ for the Sulphur Point Formation and +1.49 to +2.4‰ for the Keg River Formation. SD displayed $^{87}Sr/^{86}Sr$ values that lie between 0.7084 and 0.7102 for the Sulphur Point Formation and one value of 0.7099 for the Keg River Formation.

## Mineralized dolomite

$\delta^{18}O$ and $\delta^{13}C$ values of the mineralized CCD and SD from the Great Slave Reef, Hay West, Windy Point, and Qito properties are similar at any given locality. Their $\delta^{18}O$ values range from -12.9 to -8.4‰ (Fig. 7a and Table 3) and $\delta^{13}C$ values range from -2.4 to +2.3‰ (Fig. 7a and Table 3) with no obvious co-variance between $\delta^{13}C$ and $\delta^{18}O$ values. The $\delta^{18}O$ values are much lower than $\delta^{18}O$ values estimated for Middle Devonian dolomite, and $\delta^{13}C$ values are similar to or slightly lower than Middle Devonian dolomite (Fig. 7a). Most of the $\delta^{13}C$ and $\delta^{18}O$ values for the mineralized CCD and SD from the eastern Presqu'ile barrier are within the range of values published for the nonmineralized SD and CCD of the eastern Presqu'ile barrier (Fig. 7a), which suggests that they formed from fluids with similar $\delta^{13}C$ and $\delta^{18}O$ composition. $^{87}Sr/^{86}Sr$ ratios of the mineralized CCD and SD from the eastern Presqu'ile barrier range from 0.7081 to 0.7105 (Table 3) and do not depart greatly from that of Middle Devonian seawater (0.7077–0.7082; Veizer et al., 1999). On the $\delta^{18}O_{PDB}$ vs. $^{87}Sr/^{86}Sr$ cross plot (Fig. 7b), most of the mineralized dolomite samples from the eastern Presqu'ile barrier plot within the field defined by the nonmineralized CCD and SD of the eastern Presqu'ile barrier. The same is observed on the $\delta^{13}C_{PDB}$ vs. $^{87}Sr/^{86}Sr$ cross plot (Fig. 7c).

Four mineralized SD and CCD samples from the WCSB that come from the Slavey Creek area, adjacent to the McDonald–Hay River Fault, have slightly higher $\delta^{13}C$ values but similar $\delta^{18}O$ values compared with the eastern Presqu'ile barrier. These samples have $\delta^{18}O$ and $\delta^{13}C$ values similar to the Keg River Formation of the Rainbow field, which is also located proximal to the McDonald–Hay River Fault. $^{87}Sr/^{86}Sr$ ratios of the mineralized CCD and SD from

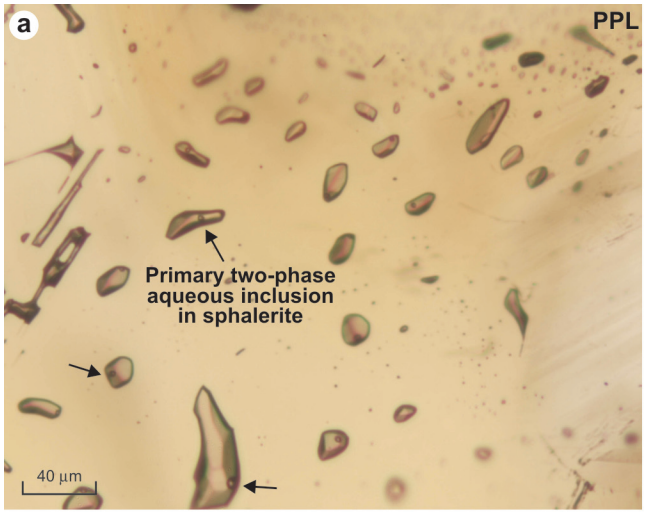


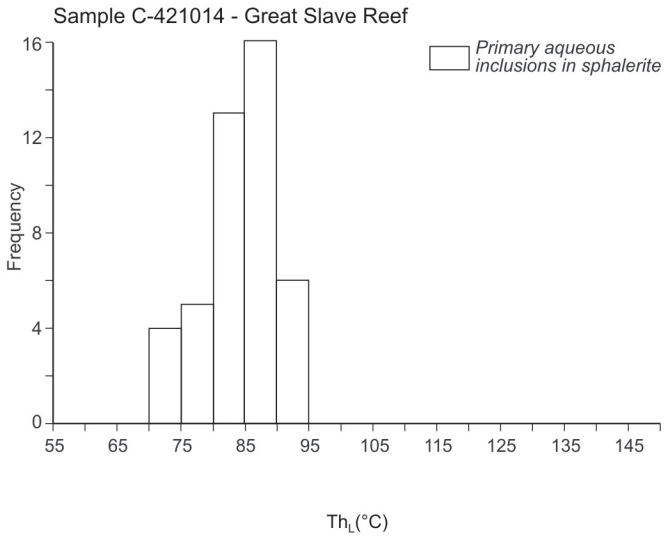



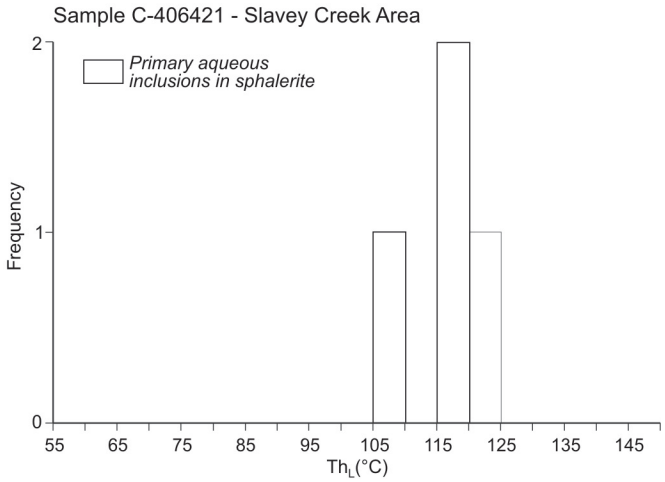


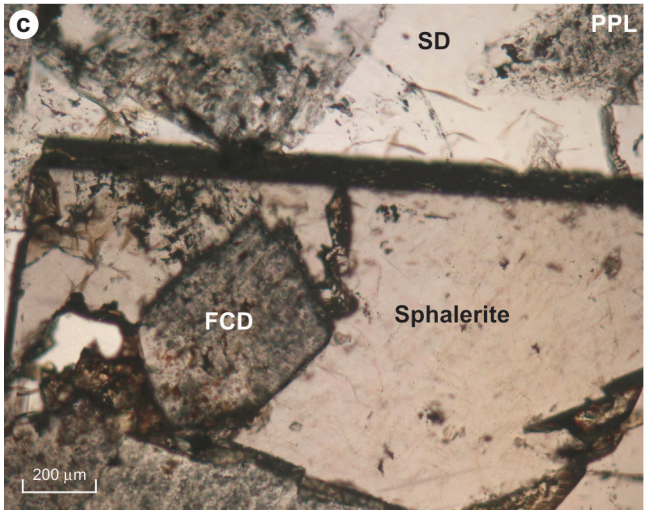


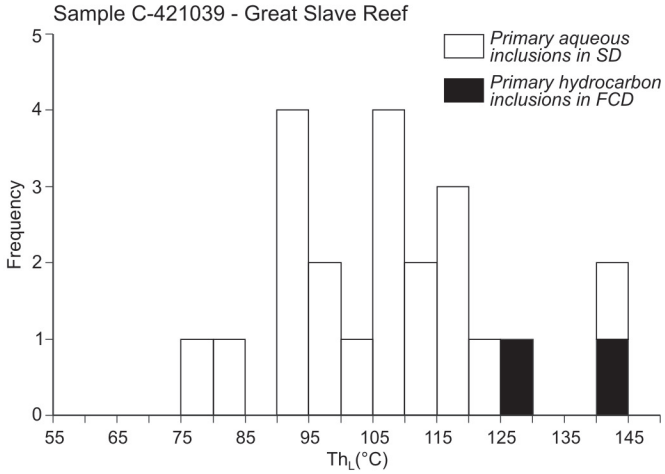


**Figure 6.** Photomicrographs of fluid inclusions and histograms showing the distribution of homogenization temperatures to liquid phase ($Th_L$). Scales as indicated. **a.** Sample C-421014 – Great Slave Reef property, orebody x25: Primary two-phase aqueous inclusions in the core of sphalerite crystal homogenized between 70 and 95°C; derived from high-salinity (29–34 wt.% NaCl equiv.) NaCl-$CaCl_2$ fluids. **b.** Sample C-406241 – Slavey Creek area: Primary two-phase aqueous inclusions in sphalerite core homogenized between 105 and 125°C; these inclusions are from the same fluid inclusion assemblage (FIA). **c.** Sample C-421039 – Great Slave Reef property, orebody O556: Primary two-phase petroleum inclusions in fine-crystalline dolomite (FCD) homogenized between 125 and 145°C; overgrown by saddle dolomite (SD) that formed at lower temperatures (~75–145°C; ave. = 103°C ± 15.4, n =20) and from high-salinity (17–32 wt.% NaCl equiv.) NaCl-$CaCl_2$ fluids.

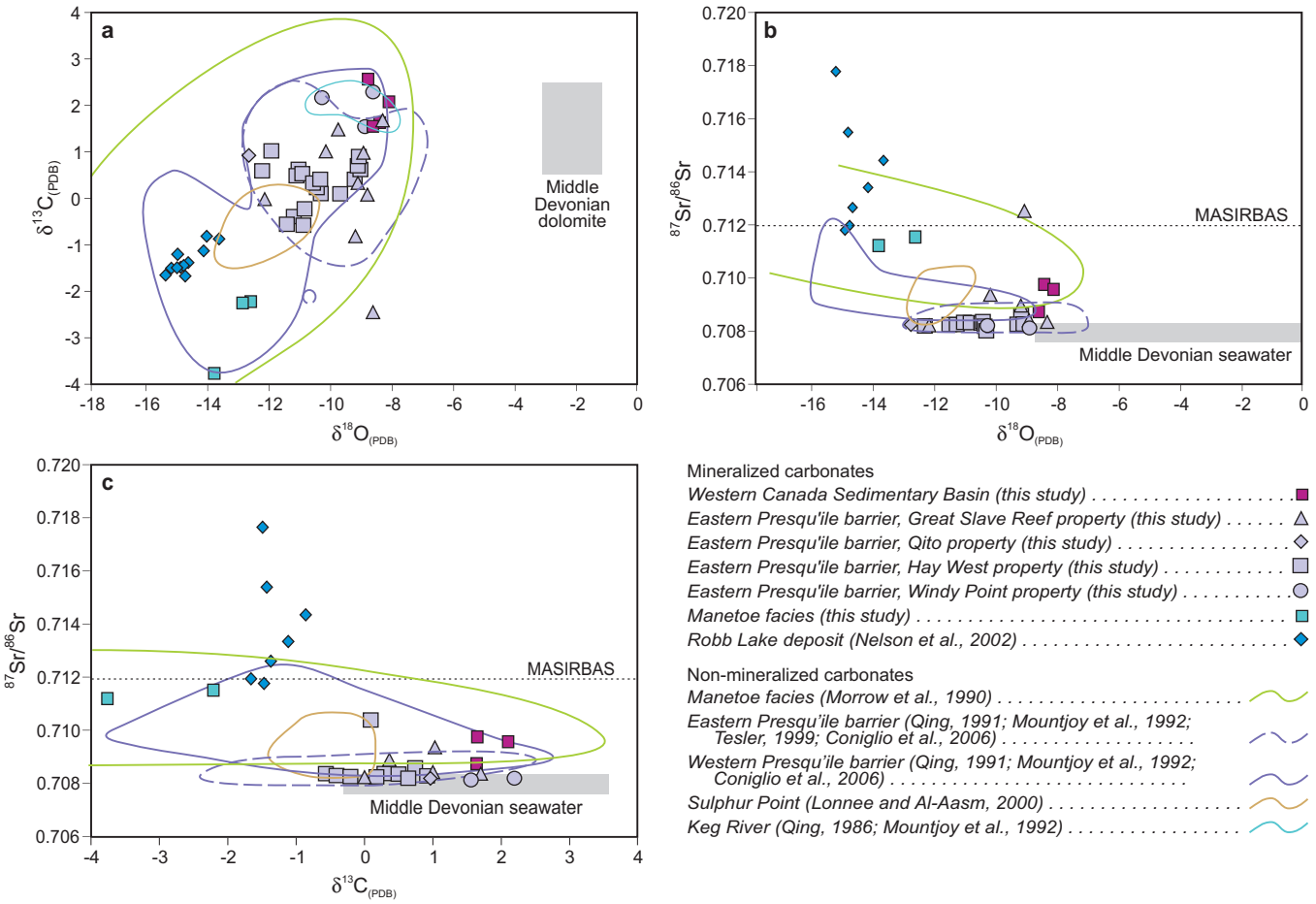


**Figure 7.** Stable carbon and oxygen and radiogenic strontium isotope data from mineralized saddle and coarse-crystalline dolomite from the Great Slave Reef, Hay West, Windy Point, and Qito properties within the eastern Presqu'ile barrier of the Western Canada Sedimentary Basin (WCSB), the Robb Lake deposit in the northern Rocky Mountains, and Manetoe facies in the Mackenzie Mountains of Yukon and NWT. These are compared to published data of nonmineralized carbonate from the eastern and western Presqu'ile barrier, the Manetoe facies, and the Sulphur Point and Keg River formations in the WCSB. **a.** $\delta^{18}O_{PDB}$ vs. $\delta^{13}C_{PDB}$; Middle Devonian dolomite values are from Hurley and Lohmann (1989). **b.** $\delta^{18}O_{PDB}$ vs. $^{87}Sr/^{86}Sr$. **c.** $\delta^{13}C_{PDB}$ vs. $^{87}Sr/^{86}Sr$. Middle Devonian seawater values are from Veizer et al. (1999). Maximum Sr isotope ratio of basinal shale (MASIRBAS) is from Machel and Cavell (1999). *See* Figures 1 to 4 for sample locations and Table 1 for analyses.

**Table 1.** Carbon, oxygen, and strontium isotope values of coarse-crystalline dolomite and saddle dolomite analyzed in this study

| Sample # | Location/Deposit | Orebody/Zone | Well/DDH number | Depth (m) | UTM Zone | Easting (NAD 83) | Northing (NAD 83) | Description of sample | Dolomite type | $\delta^{13}C_{PDB}$ | $\delta^{18}O_{PDB}$ | $\delta^{18}O_{SMOW}$ | $^{87}Sr/^{86}Sr$ |
|---|---|---|---|---|---|---|---|---|---|---|---|---|---|
| 11-2 | Robb Lake deposit | Canyon Zone | | Surface | 10 | 456710 | 6309600 | Cg white sparry dolomite in concordant mineralized breccia | CCD | -0.86 | -13.81 | 16.68 | 0.71444 |
| 11-4 | Robb Lake deposit | Canyon Zone | | Surface | 10 | 456710 | 6309600 | Cg white sparry dolomite | CCD | -1.37 | -14.83 | 15.62 | 0.71267 |
| 1B-5 | Robb Lake deposit | Lower Zone | | Surface | 10 | 456710 | 6309600 | Cg white sparry dolomite in rubble mineralized breccia | CCD | -1.12 | -14.32 | 16.15 | 0.71342 |
| 2-2(2) | Robb Lake deposit | Upper Zone | | Surface | 10 | 456710 | 6309600 | Cg sparry dolomite in mosaic mineralized breccia | CCD | -1.49 | -15.39 | 15.04 | 0.71779 |
| 3-5 | Robb Lake deposit | Waterfall Zone | | Surface | 10 | 456710 | 6309600 | Cg white sparry dolomite in mosaic mineralized breccia | CCD | -1.66 | -14.93 | 15.52 | 0.71199 |
| 72-4(2) | Robb Lake deposit | Downstream Zone | | Surface | 10 | 456710 | 6309600 | Cg white sparry dolomite in vein | CCD | -1.64 | -15.58 | 14.85 | |
| 73RGV-38 | Robb Lake deposit | Webb Ridge Zone | | Surface | 10 | 456710 | 6309600 | Cg white sparry dolomite | CCD | -1.47 | -15.08 | 15.37 | 0.71181 |
| 7-5 | Robb Lake deposit | TGS Zone | | Surface | 10 | 456710 | 6309600 | Cg white sparry dolomite in rubble mineralized breccia | CCD | -1.43 | -14.98 | 15.47 | 0.71550 |
| 7-6 | Robb Lake deposit | TGS Zone | | Surface | 10 | 456710 | 6309600 | Cg white sparry dolomite in crackle mineralized breccia | CCD | -0.80 | -14.22 | 16.25 | |
| 84-80 | Robb Lake deposit | Webb Ridge Zone | | Surface | 10 | 456710 | 6309600 | Cg white sparry dolomite in crackle mineralized breccia | CCD | -1.48 | -15.20 | 15.24 | |
| 98JN3-1(1) | Robb Lake deposit | Canyon Zone | | Surface | 10 | 456710 | 6309600 | White sparry dolomite in rubble mineralized breccia | CCD | -1.19 | -15.18 | 15.27 | |
| C-406238-1 | Slavey Creek area | | 16-34-118-21W5 | 1281.6 | 11 | 472937 | 6573428 | Cg white sparry dolomite filling fractures; associated with py | CCD | 2.10 | -8.19 | 22.42 | 0.70958 |
| C-406239-2 | Slavey Creek area | | 16-34-118-21W5 | 1281.8 | 11 | 472937 | 6573428 | Cg white sparry dolomite filling fractures; associated with py | CCD | 1.65 | -8.50 | 22.10 | 0.70977 |
| C-406242 cg | Slavey Creek area | | 16-34-118-21W5 | 1281.5 | 11 | 472937 | 6573428 | Cg white sparry dolomite filling fractures; associated with py | CCD | 2.59 | -8.88 | 21.71 | |
| C-406242-2 | Slavey Creek area | | 16-34-118-21W5 | 1281.5 | 11 | 472937 | 6573428 | Cg white sparry dolomite filling fractures; associated with py | CCD | 1.64 | -8.68 | 21.91 | 0.70874 |
| C-421175 | Zama Lake area | | 9-5-114-8-W6 | 1699.8 | 11 | 367328 | 6528063 | Mix of fg white dolomite and SD in cavities; cavities also contain ga and sph; traces of hydrocarbons along cleavage of SD | SD | | | | 0.71083 |
| C-421012 cg | Great Slave Reef | Z-155 | 223 | 101.3 | 11 | 608886 | 6736709 | Cg to mg white sparry dolomite filling veins and breccias; Ga, Sph, native sulphur, anhydrite, and late calcite fill spaces between fragments | CCD | 1.70 | -8.40 | 22.20 | 0.70836 |
| C-421014 | Great Slave Reef | X-25 | 77 | 135.4–136.6 | 11 | 606400 | 6735888 | White saddle dolomite associated with euhedral to subhedral honey-coloured sph and euhedral to anhedral ga | SD | 1.00 | -9.00 | 21.58 | 0.70842 |
| C-421021 white dolomite | Great Slave Reef | V-46 | 239 | 122.3 | 11 | 604630 | 6736261 | White saddle dolomite associated with aggregates of euhedral to subhedral sph and cg euhedral ga (intergrown with sph) | SD | 0.00 | -12.30 | 18.18 | 0.70822 |

All Sr isotopic data are presented relative to a value of 0.710245 for the NIST Sr isotopic standard SRM987; data are corrected for variable mass fractionation to a value of 0.1194 for $^{86}Sr/^{88}Sr$.

Uncertainty in $^{87}Sr/^{86}Sr$ is expressed as ± 2 sigma of the mean (2sm), equivalent to 2 standard errors (2SE).

All results for carbon and oxygen isotopes are reported in the usual per mil notation relative to the PDB standard; precision and accuracy is plus/minus 0.2 per mil for $\delta^{13}C$ and $\delta^{18}O$, respectively.

Results from the Robb Lake deposit were published in Nelson et al. (2002).

Sample location see Figures 1, 2, 3, and 4.

CCD = coarse-crystalline dolomite; MCD = medium-crystalline dolomite; SD = saddle dolomite; cg = coarse grained; mg = medium grained; sph = sphalerite; ga = galena; py = pyrite

Contents

**Table 1.** (cont.)

| Sample # | Location/Deposit | Orebody/Zone | Well/DDH number | Depth (m) | UTM Zone | Easting (NAD 83) | Northing (NAD 83) | Description of sample | Dolomite type | $\delta^{13}C_{PDB}$ | $\delta^{18}O_{PDB}$ | $\delta^{18}O_{SMOW}$ | $^{87}Sr/^{86}Sr$ |
|---|---|---|---|---|---|---|---|---|---|---|---|---|---|
| C-421023 | Great Slave Reef | V-46 | 239 | 124.1 | 11 | 604630 | 6736261 | Sparry dolomite followed by saddle dolomite filling voids in mineralized breccia (botryoidal sph and mg ga) | CCD-SD | 0.35 | -9.22 | 21.36 | 0.70893 |
| C-421053 white dolomite | Great Slave Reef | P-499 | 783 | 121.4 | 11 | 600330 | 6733565 | SD and sulphides form the groundmass of breccia | SD | 1.03 | -10.28 | 20.26 | 0.70936 |
| C-421062 clear dolomite | Great Slave Reef | W-19 | 219 | 141.8–143.4 | 11 | 605713 | 6735862 | Whitish to pinkish (clear) SD associated with colloform sph and ga in vugs | SD | -2.44 | -8.72 | 21.87 | |
| C-421062 grey dolomite | Great Slave Reef | W-19 | 219 | 141.8–143.4 | 11 | 605713 | 6735862 | Cg to mg bluish grey dolomite mixed with white CCD | CCD-MCD | 1.43 | -9.87 | 20.69 | |
| C-421062-1 | Great Slave Reef | W-19 | 219 | 141.8–143.4 | 11 | 605713 | 6735862 | Cg whitish to pinkish (clear) dolomite associated with colloform sph and ga in vugs | CCD | -0.80 | -9.30 | 21.27 | |
| C-421062-2 | Great Slave Reef | W-19 | 219 | 141.8–143.4 | 11 | 605713 | 6735862 | Cg to mg bluish grey dolomite associated with white CCD | CCD-MCD | 0.16 | -8.76 | 21.83 | |
| C-421221-1 | Windy Point | | Z29 | 49.8 | 11 | 547073 | 6790417 | Oil-stained whitish saddle dolomite associated with ga | SD | 2.31 | -8.74 | 21.85 | |
| C-421222-2 | Windy Point | | Z23 | 59 | 11 | 546503 | 6791087 | White SD in vugs associated with disseminated ga crystals (4–5 mm) | SD | 1.56 | -8.99 | 21.59 | 0.70813 |
| C-421227-1 | Windy Point | | Z25 | 46 | 11 | 546573 | 6791337 | White saddle dolomite (traces of bitumen) filling vugs; minor cg galena | SD | 2.19 | -10.41 | 20.13 | 0.70820 |
| C-421229-1 | Qito | | Q5 | 4.2 | 11 | 557978 | 6828518 | Saddle dolomite replacing matrix dolomite and forming cement in fractures and breccias; associated with sph | SD | 0.97 | -12.88 | 17.58 | 0.70824 |
| C-421230-1 | Hay West | | HW-80-29 | 547.7 | 11 | 520962 | 6736247 | White/ bluish grey sparry dolomite with disseminated cg euhedral sph (1 cm-size to several mm - 10%) and ga | CCD | 0.52 | -11.23 | 19.28 | 0.70834 |
| C-421230-2 | Hay West | | HW-80-29 | 547.7 | 11 | 520962 | 6736247 | Cg white dolomite associated with sph and ga | CCD | 0.65 | -9.20 | 21.38 | 0.70823 |
| C-421230-3 | Hay West | | HW-80-29 | 547.7 | 11 | 520962 | 6736247 | White saddle dolomite-lined cavities; associated with cg euhedral sph | SD | 0.91 | -9.21 | 21.37 | 0.70827 |
| C-421231-1 | Hay West | | HW-80-29 | 544.7 | 11 | 520962 | 6736247 | White saddle dolomite with traces of ga and sph | SD | 0.72 | -9.24 | 21.33 | 0.70852 |
| C-421234-1 | Hay West | | HW-79-9 | 496.5 | 11 | 541650 | 6717585 | Cg white replacive dolomite forms pseudobreccia and fills vugs | CCD | 0.23 | -10.54 | 19.99 | 0.70832 |
| C-421235-2 | Hay West | | HW-81-50 | 327.5 | 11 | 559522 | 6724511 | Cg white replacive dolomite forms pseudobreccia | CCD | 0.53 | -11.09 | 19.43 | 0.70828 |
| C-421236-2 | Hay West | | HW-80-31 | 566.8–567.5 | 11 | 522292 | 6732028 | White saddle dolomite lining fractures and walls of cavities; associated with fg sph | SD | 0.42 | -9.37 | 21.20 | 0.70829 |
| C-421237-2 | Hay West | | HW-80-31 | 573.6–574.5 | 11 | 522292 | 6732028 | White saddle dolomite lining fractures; associated with fg disseminated sph | SD | 0.12 | -10.44 | 20.10 | 0.70821 |
| C-421238-1 | Hay West | | HW-80-14 | 413.5 | 11 | 541450 | 6724395 | Cg white sparry dolomite cement in fragmental breccia | CCD | 0.39 | -10.60 | 19.93 | 0.70826 |
| C-421239-2 | Hay West | | HW-79-11 | 573–574.8 | 11 | 521206 | 6741163 | White to clear saddle dolomite associated with small sph crystal in vug | SD | 0.62 | -12.39 | 18.09 | 0.70820 |
| C-421240-2 | Hay West | | HW-80-20 | 326.8 | 11 | 540218 | 6738513 | White saddle dolomite filling vugs and fractures; traces of sulphur | SD | 0.34 | -10.68 | 19.85 | 0.70819 |

**Table 1.** (cont.)

| Sample # | Location/Deposit | Orebody/Zone | Well/DDH number | Depth (m) | UTM Zone | Easting (NAD 83) | Northing (NAD 83) | Description of sample | Dolomite type | $\delta^{13}C_{PDB}$ | $\delta^{18}O_{PDB}$ | $\delta^{18}O_{SMOW}$ | $^{87}Sr/^{86}Sr$ |
|---|---|---|---|---|---|---|---|---|---|---|---|---|---|
| C-421241-1 | Hay West | | HW-80-26 | 306.8 | 11 | 558058 | 6728465 | Cg brownish sparry dolomite | CCD | -0.57 | -11.05 | 19.47 | 0.70832 |
| C-421241-2 | Hay West | | HW-80-26 | 306.8 | 11 | 558058 | 6728465 | Cg white sparry dolomite | CCD | -0.40 | -11.39 | 19.12 | 0.70824 |
| C-421241-3 | Hay West | | HW-80-26 | 306.8 | 11 | 558058 | 6728465 | White/clear SD (with traces of white sparry dolomite) in vugs | SD | -0.53 | -11.60 | 18.90 | 0.70828 |
| C-421242-1 | Hay West | | HW-80-18 | 372.8 | 11 | 540784 | 6733563 | Zebra-looking texture in brownish cg sparry dolomite with darker sparry dolomite with snow-on-roof texture | CCD | 0.63 | -11.17 | 19.35 | |
| C-421242-2 | Hay West | | HW-80-18 | 372.8 | 11 | 540784 | 6733563 | White saddle dolomite in veins crosscut brownish and grey MCD | SD | 0.38 | -10.51 | 20.03 | |
| C-421244-2 | Hay West | | HW-81-45 | 323.9 | 11 | 528291 | 6746545 | Cg white dolomite cement in breccia and open spaces | CCD | 1.04 | -12.08 | 18.41 | |
| C-421245-2 | Hay West | | HW-81-47 | 308.3 | 11 | 549764 | 6736919 | White saddle dolomite in crackle breccia (traces of bitumen and py) | SD | 0.10 | -9.81 | 20.75 | 0.71045 |
| C-421246-2 | Hay West | | HW-81-41 | 292.5 | 11 | 544932 | 6750245 | White saddle dolomite (traces of clear saddle dolomite?) and sulphides in vugs | SD | -0.20 | -10.98 | 19.54 | 0.70824 |
| C-433001-2 | Mount Ebbut area | Manetoe facies | D-50-62-20-122-15 | 659 | 10 | 530947 | 6909642 | White saddle dolomite and white sparry dolomite associated with sph in fractures and veins | SD | -3.76 | -13.97 | 16.46 | 0.71123 |
| C-433002-1 | Cli Lake area | Manetoe facies | M-05-62-00-123-00 | 1489.3 | 10 | 498357 | 6864845 | White saddle dolomite cement and sph crystals as fracture- and vein-filling cement | SD | -2.21 | -12.76 | 17.71 | 0.71156 |
| C-433002-2 | Cli Lake area | Manetoe facies | M-05-62-00-123-00 | 1489.3 | 10 | 498357 | 6864845 | White saddle dolomite cement and sph crystals as fracture- and vein-filling cement | SD | -2.24 | -13.03 | 17.43 | |

All Sr isotopic data are presented relative to a value of 0.710245 for the NIST Sr isotopic standard SRM987; data are corrected for variable mass fractionation to a value of 0.1194 for $^{86}Sr/^{88}Sr$.

Uncertainty in $^{87}Sr/^{86}Sr$ is expressed as ± 2 sigma of the mean (2sm), equivalent to 2 standard errors (2SE).

All results for carbon and oxygen isotopes are reported in the usual per mil notation relative to the PDB standard; precision and accuracy is plus/minus 0.2 per mil for $\delta^{13}C$ and $\delta^{18}O$, respectively.

Results from the Robb Lake deposit were published in Nelson et al. (2002).

Sample location see Figures 1, 2, 3, and 4.

CCD = coarse-crystalline dolomite; MCD = medium-crystalline dolomite; SD = saddle dolomite; cg = coarse grained; mg = medium grained; sph = sphalerite; ga = galena; py = pyrite

Contents

**Table 2.** Range and average isotopic values of nonmineralized coarse-crystalline dolomite and saddle dolomite from the Western Canada Sedimentary Basin and the northern Canadian Rocky Mountains

| Formation, facies, area | $\delta^{18}O_{PDB}$ | | | | $\delta^{13}C_{PDB}$ | | | | $^{87}Sr/^{86}Sr$ | | | | Sources |
|---|---|---|---|---|---|---|---|---|---|---|---|---|---|
| | Range | Mean | n | Std. Dev. | Range | Mean | n | Std. Dev. | Range | Mean | n | Std. Dev. | |
| Eastern Presqu'ile barrier | | | | | | | | | | | | | |
| CCD | -12.44 to -7.62 | -9.35 | 34 | 1.28 | -1.42 to 1.78 | 0.25 | 34 | 0.82 | 0.70816 to 0.70880 | 0.7085 | 5 | 0.0003 | Qing (1991), Mountjoy et al. (1992) |
| SD | -13.0 to -7.03 | -9.65 | 73 | 1.47 | -2.24 to +2.5* | 0.53 | 72 | 0.92 | 0.70807 to 0.70877 | 0.7083 | 25 | 0.0002 | Qing (1991), Mountjoy et al. (1992), Tesler (1999), Coniglio et al. (2006) |
| Western Presqu'ile barrier | | | | | | | | | | | | | |
| CCD | -15.84 to -10.41 | -13.70 | 18 | 1.58 | -3.80 to 1.41 | -0.92 | 18 | 1.37 | 0.70859 to 0.71211 | 0.7102 | 9 | 0.0013 | Qing (1991), Mountjoy et al. (1992), Tesler (1999) |
| SD | -16.01 to -8.7 | -12.82 | 29 | 1.92 | -3.65 to 2.70 | -0.99 | 29 | 1.40 | 0.7085 to 0.7106 | 0.7093 | 16 | 0.0006 | Qing (1991), Mountjoy et al. (1992), Tesler (1999), Coniglio et al. (2006) |
| Sulphur Point Fm, NW Alberta | | | | | | | | | | | | | |
| SD | -13.68 to -10.71 | -12.02 | 27 | 0.77 | -1.44 to 0.18 | -0.49 | 27 | 0.42 | 0.70839 to 0.71024 | 0.7093 | 6 | 0.0008 | Lonnee and Al-Aasm (2000) |
| Keg River Fm, NW Alberta | | | | | | | | | | | | | |
| SD | -10.65 to -7.84 | -9.15 | 22 | 0.77 | 1.49 to 2.35 | 1.97 | 22 | 0.21 | 0.709900 | | 1 | | Qing (1986), Mountjoy et al. (1992) |
| Manetoe facies, SW NWT | | | | | | | | | | | | | |
| SD-CCD | -17.33 to -7.70 | -11.28 | 135 | 2.87 | -7.35 to 3.53 | -1.40 | 135 | 1.36 | 0.70906 to 0.71282 | 0.7099 | 10 | 0.00350 | Morrow et al. (1990) |

CCD: coarse-crystalline dolomite; SD: saddle dolomite.
* The range does not include the value of +11.8 of Coniglio et al. (2006).

**Table 3.** Range and average isotopic values of mineralized coarse-crystalline dolomite and saddle dolomite analyzed in this study

| | $\delta^{18}O_{PDB}$ | | | | $\delta^{13}C_{PDB}$ | | | | $^{87}Sr/^{86}Sr$ | | | |
|---|---|---|---|---|---|---|---|---|---|---|---|---|
| **Location/Deposit** | **Range** | **Mean** | **n** | **Std. Dev.** | **Range** | **Mean** | **n** | **Std. Dev.** | **Range** | **Mean** | **n** | **Std. Dev.** |
| Robb Lake | | | | | | | | | | | | |
| CCD | -15.58 to -13.81 | -14.87 | 11 | 0.54 | -1.66 to -0.8 | -1.32 | 11 | 0.29 | 0.71181 to 0.71779 | 0.71395 | 7 | 0.00215 |
| WCSB | | | | | | | | | | | | |
| CCD | -8.88 to -8.19 | -8.56 | 4 | 0.29 | 1.64 to 2.59 | 2.00 | 4 | 0.45 | 0.70874 to 0.70977 | 0.70936 | 3 | 0.00055 |
| SD | | | | | | | | | 0.71083 | 0.71083 | 1 | |
| Manetoe facies | | | | | | | | | | | | |
| SD | -13.97 to -12.76 | -13.25 | 3 | 0.64 | -3.76 to -2.21 | -2.74 | 3 | 0.89 | 0.71123 to 0.71156 | 0.71139 | 2 | 0.00023 |
| Great Slave Reef | | | | | | | | | | | | |
| CCD (-MCD) | -9.87 to -8.4 | -9.08 | 4 | 0.64 | -0.8 to 1.7 | 0.62 | 4 | 1.16 | 0.70836 | 0.70836 | 1 | |
| CCD-SD | -9.22 | -9.22 | 1 | | 0.35 | 0.35 | 1 | | 0.70893 | 0.70893 | 1 | |
| SD | -12.3 to -8.72 | -10.08 | 4 | 1.63 | -2.44 to 1.03 | -0.10 | 4 | 1.63 | 0.70822 to 0.70936 | 0.70867 | 3 | 0.00056 |
| Windy Point | | | | | | | | | | | | |
| SD | -10.41 to -8.74 | -9.38 | 3 | 0.90 | 1.56 to 2.31 | 2.02 | 3 | 0.40 | 0.70813 to 0.70820 | 0.70817 | 2 | 0.00000 |
| Hay West | | | | | | | | | | | | |
| CCD | -12.08 to -9.20 | -10.93 | 9 | 0.79 | -0.57 to 1.04 | 0.34 | 9 | 0.52 | 0.70823 to 0.70834 | 0.70828 | 7 | 0.00004 |
| SD | -12.39 to -9.21 | -10.42 | 10 | 1.05 | -0.53 to 0.91 | 0.29 | 10 | 0.43 | 0.70819 to 0.71045 | 0.70852 | 9 | 0.00073 |
| Qito | | | | | | | | | | | | |
| SD | -12.88 | -12.88 | 1 | | 0.97 | 0.97 | 1 | | 0.708238 | 0.70824 | 1 | |
| Eastern Presqu'ile barrier | | | | | | | | | | | | |
| CCD (-MCD) | -12.08 to -8.4 | -10.36 | 13 | 1.14 | -0.8 to 1.7 | 0.42 | 13 | 0.73 | 0.70823 to 0.70836 | 0.70829 | 8 | 0.00005 |
| SD | -12.88 to -8.72 | -10.31 | 18 | 1.31 | -2.44 to 2.31 | 0.53 | 18 | 1.06 | 0.70813 to 0.71045 | 0.70848 | 15 | 0.00062 |
| CCD-SD | -9.22 | -9.22 | 1 | | 0.35 | 0.35 | 1 | | 0.70893 | 0.70893 | 1 | |
| CCD (-MCD) +SD | -12.88 to -8.4 | -10.30 | 32 | 1.22 | -2.44 to 2.31 | 0.48 | 32 | 0.91 | 0.70813 to 0.71045 | 0.70844 | 24 | 0.00050 |

The Eastern Presqu'ile barrier data includes the Great Slave Reef, Windy Point, Qito, and Hay West properties.
MCD: medium-crystalline dolomite; CCD: coarse-crystalline dolomite; SD: saddle dolomite.

the Slavey Creek and Zama Lake area (0.7087–0.7108; ave. = 0.7097) are slightly higher than the mineralized and nonmineralized dolomite samples from the eastern Presqu'ile barrier (0.7081–0.7105; ave. = 0.7084).

The CCD and SD associated with sulphide minerals at Robb Lake and the Manetoe facies have lower values of $\delta^{13}C$ and $\delta^{18}O$ compared to the eastern Presqu'ile barrier. At Robb Lake, values of $\delta^{18}O$ range from -15.6 to -13.8‰ and values of $\delta^{13}C$ range from -1.7 to -0.8‰ (Fig. 7a and Table 3). These values plot in the lighter part of the data set of Qing (1991), Mountjoy et al. (1992), and Coniglio et al. (2006) for the western Presqu'ile barrier (Fig. 7a). The $\delta^{18}O$ and $\delta^{13}C$ values of the mineralized SD from the Manetoe facies (Fig. 7a and Table 3) overlap the lighter values for the nonmineralized dolomite of the Manetoe facies (Fig. 7a and Table 2), which show a considerable scatter of $\delta^{18}O$ (-17.3 to -7.7‰) and $\delta^{13}C$ (-7.4 to +3.5‰) values (Morrow et al., 1990). Significantly radiogenic strontium is found in CCD and SD of the Robb Lake deposit (0.7118–0.7178), and mineralized SD of the Manetoe facies (0.7112–0.7116; Table 3). The late-stage dolostone-hosted saddle dolomite and calcite cements of the Swan Hills Formation near the western margin of the WCSB also have radiogenic strontium values of 0.7088 to 0.7370 (Wendte et al., 1998; Duggan et al., 2001). Mountjoy et al. (1992) report $^{87}Sr/^{86}Sr$ ratios of 0.7090 to 0.7121 in the deep subsurface dolomite and a slightly lower value (0.7086) in the shallow subsurface dolomite of the western Presqu'ile barrier. On the $^{18}O_{PDB}$ and $^{13}C_{PDB}$ vs. $^{87}Sr/^{86}Sr$ plots (Fig. 7b, c), the Robb Lake samples define a marked, steep departure to radiogenic Sr from the shallow trend defined by the mineralized and nonmineralized carbonate of the eastern and western Presqu'ile barrier. The mineralized Manetoe SD is within the upper range of values published for the nonmineralized Manetoe dolomite (0.7091–0.7128; Morrow et al., 1990).

## Isotopic trends

On the cross plots of $\delta^{18}O$ vs. longitude (Fig. 8a), $\delta^{13}C$ vs. longitude (Fig. 8b), and $^{87}Sr/^{86}Sr$ vs. longitude (Fig. 8c), the values of mineralized and nonmineralized CCD and SD are fairly constant along the length of the eastern Presqu'ile barrier. The nonmineralized CCD and SD in the western Presqu'ile barrier shows that in spite of the fact that there is a wide variation of $\delta^{18}O$ values at certain longitudes, there is a broad overall westward decreasing trend (Fig. 8a). For example, at approximately 117.2°W, $\delta^{18}O$ values range from -12.0 to -8.7‰, and at approximately 121°W, $\delta^{18}O$ values range from -15.8 to -13.0‰. No data on mineralized dolomites are available within the western Presqu'ile barrier (i.e. between 117 and 122°W) to verify the change in isotopic values versus longitude. In the Rocky and Mackenzie mountains, mineralized CCD and SD of the Manetoe facies and the Robb Lake deposit have low $\delta^{18}O$ values (-15.6 to -12.8; Fig. 8a), similar to deep subsurface nonmineralized CCD and SD of the western Presqu'ile barrier (-16.0 to -12.8‰; Mountjoy et al., 1992). Nonmineralized SD of the Manetoe facies however, shows a considerable range of $\delta^{18}O$ values that overlap the range of values for both the eastern and the western Presqu'ile barrier (Fig. 8a), therefore showing no westward decreasing trend in $\delta^{18}O$ values along the entire length of the Presqu'ile barrier.

$\delta^{13}C$ values in mineralized and nonmineralized CCD and SD range widely along the whole length of the Presqu'ile barrier and the Rocky and Mackenzie mountains from -7.35 to +3.5‰ with no apparent spatial trend (Fig. 8b).

On the cross plot of $^{87}Sr/^{86}Sr$ vs. longitude (Fig. 8c), the $^{87}Sr/^{86}Sr$ values of the mineralized CCD and SD increase from the eastern Presqu'ile barrier to the Rocky Mountains. Moreover, $^{87}Sr/^{86}Sr$ values of the nonmineralized CCD and SD show a discernible westward increase from the eastern to the western Presqu'ile barrier (Fig. 8c). As observed for oxygen isotopes, the $^{87}Sr/^{86}Sr$ ratios of the Manetoe facies within the Rocky Mountains are similar to those of the deep subsurface dolomite of the western Presqu'ile barrier. Another interesting observation is the westward increase of $^{87}Sr/^{86}Sr$ values along the McDonald–Hay River Fault (Fig. 9), with values of 0.7081–0.7105 (ave. = 0.7084 ± 0.0004 [1σ], n=134) at Pine Point (Qing, 1991; Mountjoy et al., 1992; Coniglio et al., 2006; this study) to values of 0.7087–0.7098 (ave. = 0.7094 ± 0.0006 [1σ], n=3) at Slavey Creek (this study), 0.7108 at Zama Lake (this study), and 0.7084–0.7102 (ave. = 0.7094 ± 0.0008 [1σ], n= 7) at Rainbow field (Qing, 1986; Lonnee and Al-Aasm, 2000).

# LEAD ISOTOPES

## Description of samples

Lead isotope analyses of sphalerite and galena from the WCSB, both within and external to the Presqu'ile barrier, the Rocky Mountains, and the Mackenzie Mountains are listed in Table 4 and sample locations are plotted on Figure 10.

Galena and sphalerite samples are selected from the Great Slave Reef, Hay West, Windy Point, and Qito properties within the Slave Point, Sulphur Point, Watt Mountain, Pine Point, and Keg River formations of the eastern Presqu'ile barrier. Other galena and sphalerite samples (704, 1245, 2425, 1426, 4818, and 1904) occur in dolostone of the Slave Point and Pine Point formations along the carbonate front of the western Presqu'ile barrier. In the WCSB of Alberta, three samples (98AB3, C-406237, and C-421175) are from the Slavey Creek, Steen River, and Zama Lake areas, directly over the westerly subsurface projection of the McDonald–Hay River Fault as defined by its aeromagnetic signature. Samples 98AB4, C-406244, and C-406247 are from the Pekisko, Slave Point, and Wabamun formations, respectively, overlying the Peace River Arch. Sample C-406243 is a large galena cube found in stream sediments of the Cordillera mountain front. Samples 7350, 7808, and C-433027 are from the Jean Marie Member in the Helmet North gas field of the Cordova Embayment, a reentrant in the Presqu'ile barrier.

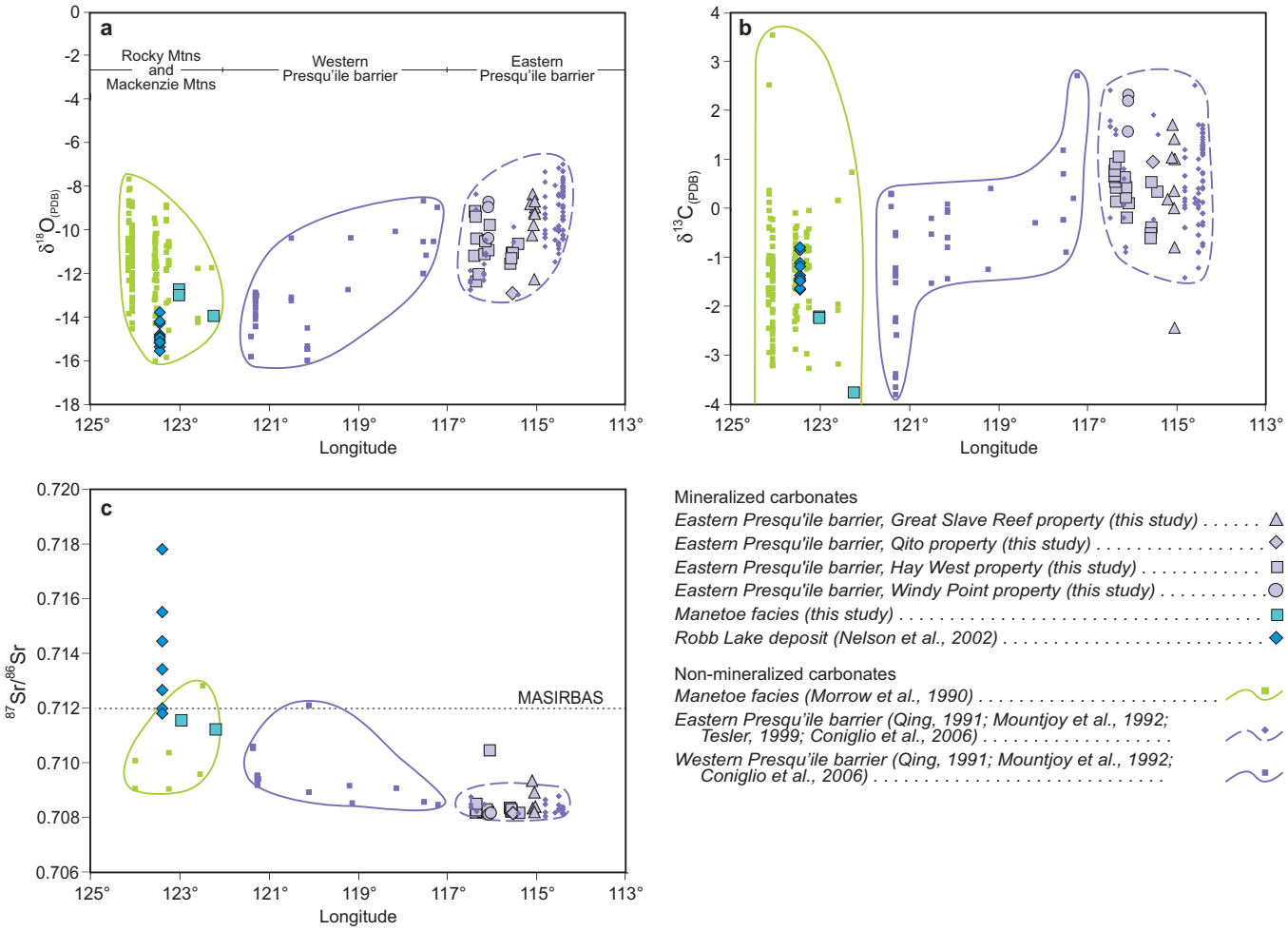


**Figure 8.** Stable and strontium isotope data vs. longitude of mineralized saddle and coarse-crystalline dolomite from the Great Slave Reef, Hay West, Windy Point, and Qito properties within the eastern Presqu'ile barrier of the Western Canada Sedimentary Basin (WCSB), the Robb Lake deposit in the northern Rocky Mountains, and Manetoe facies in the Mackenzie Mountains of Yukon and NWT. These are compared to published data of nonmineralized carbonate from the eastern and western Presqu'ile barrier and the Manetoe facies. **a.** $\delta^{18}O_{PDB}$ vs. longitude. **b.** $\delta^{13}C_{PDB}$ vs. longitude. **c.** $^{87}Sr/^{86}Sr$ vs. longitude. Longitude information for the Pine Point deposits is not accurate.

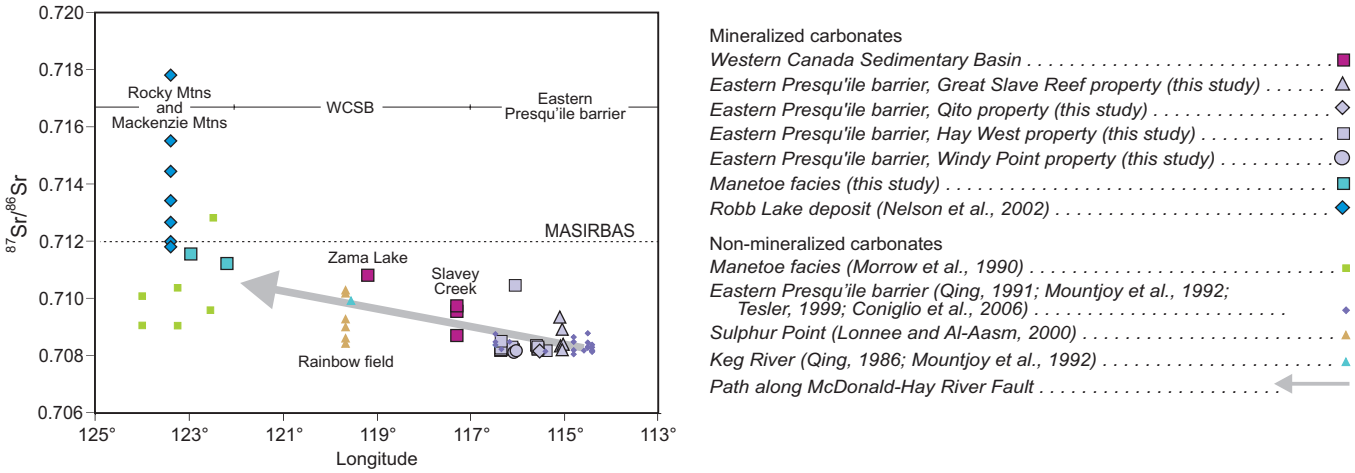


**Figure 9.** Strontium isotope ratios vs. longitude. The Slavey Creek area, Zama Lake area, and Rainbow petroleum field are situated along the McDonald–Hay River Fault. The arrow indicates the westward increase of $^{87}Sr/^{86}Sr$ ratios from the Pine Point deposits to the northern Rocky Mountains following an approximate path along the McDonald–Hay River Fault.

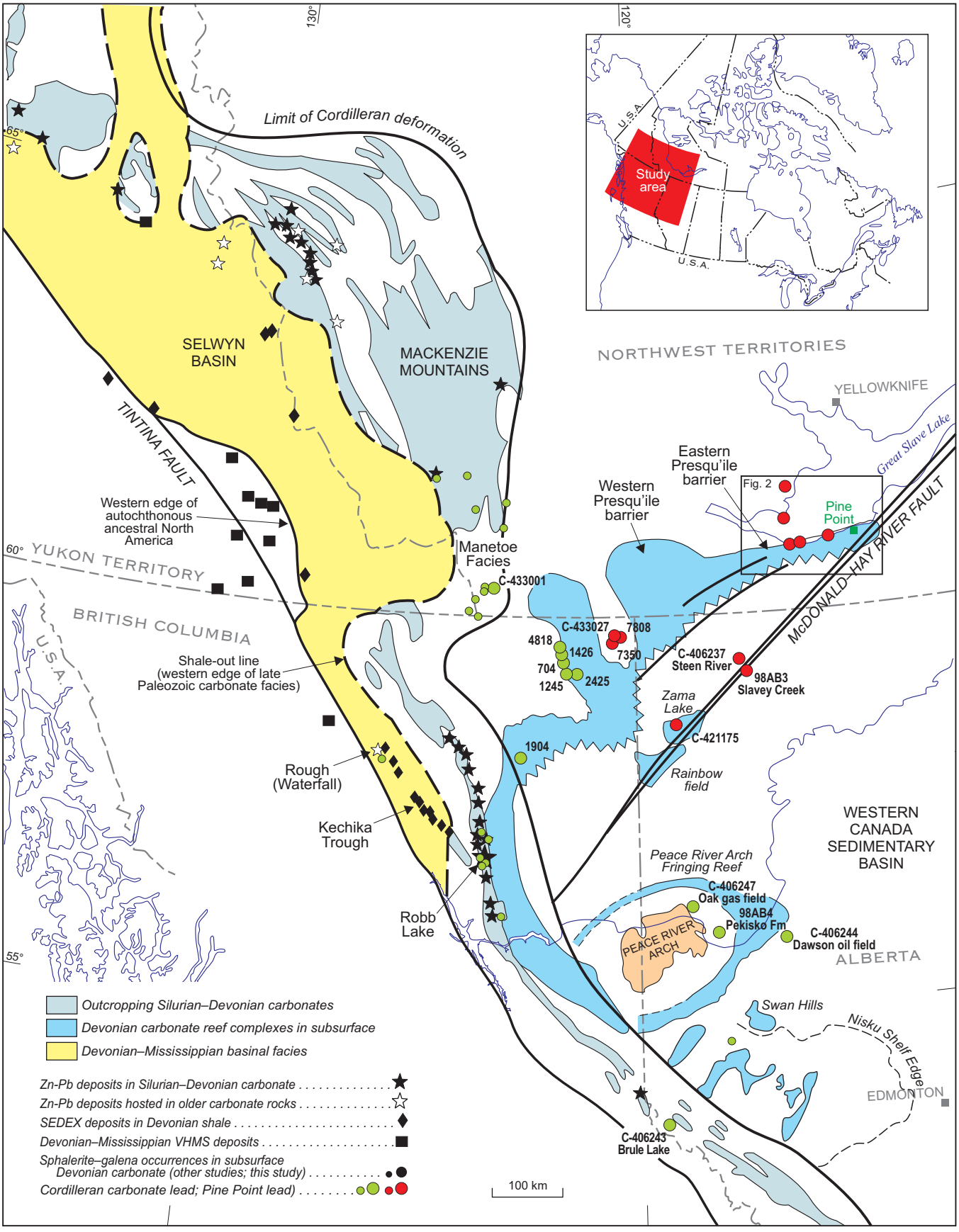


**Figure 10.** Location of samples analyzed for lead isotopes in this and other studies. Also indicated is the lead isotopic signature ("Cordilleran carbonate lead" versus "Pine Point lead") of sulphide occurrences within the Western Canada Sedimentary Basin and the northern Rocky Mountains.

**Table 4.** Lead isotope values for galena and sphalerite of mineralized carbonate samples from the Western Canada Sedimentary Basin, including the eastern and western Presqu'ile barrier, and the Manetoe facies

| Sample number | Location/Deposit | Well/DDH number | Depth (m) | UTM Zone | Easting (NAD 83) | Northing (NAD 83) | Description | Mineral | $^{206}Pb/^{204}Pb$ | $^{207}Pb/^{204}Pb$ | $^{208}Pb/^{204}Pb$ | $^{207}Pb/^{206}Pb$ | $^{208}Pb/^{206}Pb$ |
|---|---|---|---|---|---|---|---|---|---|---|---|---|---|
| 704-1 | Western Presqu'ile barrier, NE B.C. | b-68-K 94P/5 | 2096.7 | 10 | 565288 | 6593037 | Coarse Ga in vuggy recrystallized dolomite | Galena | 23.707 | 16.212 | 43.730 | 0.684 | 1.845 |
| 1245-1 | Western Presqu'ile barrier, NE B.C. | b-40-A 94P/5 | 2146.7 | 10 | 578533 | 6571601 | Coarse Ga in vein with white sparry dolomite | Galena | 20.672 | 15.899 | 40.721 | 0.769 | 1.970 |
| 1426-1 | Western Presqu'ile barrier, NE B.C. | b-99-K 94P/5 | 2124.8 | 10 | 564589 | 6595469 | Coarse brown Sph with saddle dolomite in vugs | Sphalerite | 19.239 | 15.739 | 39.486 | 0.818 | 2.052 |
| 1904-1 | Western Presqu'ile barrier, NE B.C. | d-59-K 94J/2 | 2394.8 | 10 | 508485 | 6452586 | Sph and Py-rich massive sulphide section (0.5 m thick); bedding-parallel | Sphalerite | 22.820 | 16.109 | 43.329 | 0.706 | 1.899 |
| 1904-2 | Western Presqu'ile barrier, NE B.C. | d-59-K 94J/2 | 2394.8 | 10 | 508485 | 6452586 | Ga patches in above section | Galena | 21.219 | 15.979 | 41.910 | 0.753 | 1.975 |
| 2425-2 | Western Presqu'ile barrier, NE B.C. | d-57-B 94P/5 | 2098.2 | 10 | 573666 | 6573894 | Ga cube with quartz prisms on fracture surface | Galena | 21.405 | 15.960 | 41.229 | 0.746 | 1.926 |
| 4818-1 | Western Presqu'ile barrier, NE B.C. | a-88-F 94P/12 | 2178 | 10 | 565419 | 6613389 | Ga filling small fracture that crosscuts zebra dolomite | Galena | 23.099 | 16.148 | 43.337 | 0.699 | 1.876 |
| 7350-1 | Jean Marie M, Redknife Fm/Helmet North Field - Cordova Embayment | d-37-I 94P/10 | 1141 | 10 | 636382 | 6620242 | Single Ga grain forms infilling of small vug; others are lined with dolomite | Galena | 18.267 | 15.574 | 38.148 | 0.853 | 2.088 |
| 7808-1 | Jean Marie M, Redknife Fm/Helmet North Field - Cordova Embayment | b-68-D 94P/16 | 1139 | 10 | 641784 | 6631981 | Scattered tiny Ga grains with dense secondary dolomite (minute vugs in fine grained dolomite?) | Galena | 18.296 | 15.604 | 38.230 | 0.853 | 2.090 |
| C-433027 | Jean Marie M, Redknife Fm/Helmet North Field - Cordova Embayment | b-71-J 94P/10 | 1157.0 | 10 | 632849 | 6623564 | Single Ga crystal in patchy, chalky looking dolomite | Galena | 18.538 | 15.572 | 38.389 | 0.840 | 2.071 |
| 98AB3 | Slavey Creek area | 16-34-118-21 W5 | 1286.3 | 11 | 472937 | 6573428 | Replacive pale Sph in mosaic breccia matrix with SD, pre-stylolites | Sphalerite | 18.188 | 15.592 | 38.131 | 0.857 | 2.097 |
| 98AB4 | Pekisko Fm/ Peace River Arch | 6-21-80-1 W6 | 1698.65 | 11 | 431612 | 6200572 | Tiny brown Sph grains in open spaces in small breccia zone; others are lined with pyrobitumen or filled with coarse calcite | Sphalerite | 24.252 | 16.330 | 46.248 | 0.673 | 1.907 |
| *C-433017 | Mount Gass, Highrock Range/Oldman River property | | Surface | 11 | 662534 | 5555767 | Ga veins and fine-grained white calcite cut fine-grained crystalline dolomite | Galena | 21.779 | 15.941 | 44.440 | 0.732 | 2.040 |
| *C-433018 | Mount Gass, Highrock Range/Oldman River property | | Surface | 11 | 662534 | 5555767 | Ga veins associated with white sparry dolomite and white sparry calcite | Galena | 21.778 | 15.945 | 44.454 | 0.732 | 2.041 |
| C-406237 | Steen River area | 10-22-120-1W6 | 1237.4 | 11 | 439374 | 6589455 | Ga specks (1 mm) in dolomitized patches of the Slave Point Fm | Galena | 18.174 | 15.556 | 38.101 | 0.856 | 2.096 |
| C-406243 | Brule Lake area | | Surface | 11 | 441400 | 5908450 | 1x1.2x0.5 cm crystal of Ga; found in stream sediments | Galena | 22.045 | 15.960 | 41.122 | 0.724 | 1.865 |
| C-406244 | Dawson oil field | 4-35-79-16W5 | 2072.6 | 11 | 537570 | 6193470 | Slave Point Formation at dolostone-limestone contact; 15-20% Py filling fractures; specks (1 mm) of Ga | Galena | 22.214 | 16.123 | 44.534 | 0.726 | 2.005 |
| C-406247 | Oak gas field | 11-8-83-6w6 | 2222.7 | 11 | 381079 | 6228345 | Keg River Formation; grey FCD matrix with patches of CCD and cavities filled with SD, calcite, and Sph | Sphalerite | 22.284 | 16.050 | 44.987 | 0.720 | 2.019 |
| C-421175 | Zama Lake area | 9-5-114-8-W6 | 1699.8 | 11 | 367328 | 6528063 | Fine crystals of Ga and Sph in open space cavities of breccia | Sphalerite | 18.269 | 15.601 | 38.240 | 0.854 | 2.093 |
| C-421011 | Great Slave Reef property - Z155 | 223 | 99.7 | 11 | 608886 | 6736709 | FCD and brownish dolomite cut by veinlets of CCD, native sulphur, Sph, and Ga | Galena | 18.176 | 15.593 | 38.230 | 0.858 | 2.103 |

Note: The first 11 samples were reported in a previous study by Nelson et al. (2002).
Abbreviation: M=Member, Fm=Formation, CCD=coarse-crystalline dolomite, MCD=medium-crystalline dolomite, FCD=fine-crystalline dolomite, SD=saddle dolomite, Ga=galena, Sph=sphalerite, Py=pyrite.
For sample location, see Figures 1, 2, 3, 4, and 10.
*Samples not located in Figures 1, 2, 3, 4, and 10.

**Table 4.** (cont.)

| Sample number | Location/Deposit | Well/DDH number | Depth (m) | UTM Zone | Easting (NAD 83) | Northing (NAD 83) | Description | Mineral | $^{206}Pb/^{204}Pb$ | $^{207}Pb/^{204}Pb$ | $^{208}Pb/^{204}Pb$ | $^{207}Pb/^{206}Pb$ | $^{208}Pb/^{206}Pb$ |
|---|---|---|---|---|---|---|---|---|---|---|---|---|---|
| C-421012 | Great Slave Reef property - Z155 | 223 | 101.3 | 11 | 608886 | 6736709 | Veins of white CCD, Ga, Sph, and late calcite | Galena | 18.160 | 15.578 | 38.199 | 0.858 | 2.103 |
| C-421014 | Great Slave Reef property - X25 | 77 | 135.4–136.6 | 11 | 606400 | 6735888 | Semi-massive Ga and Sph forming cm-sized bands in SD | Galena | 18.193 | 15.613 | 38.277 | 0.858 | 2.104 |
| C-421021 | Great Slave Reef property - V46 | 239 | 122.3 | 11 | 604630 | 6736261 | Coarse Ga and colloform Sph forming laminae and bands in SD | Galena | 18.157 | 15.569 | 38.159 | 0.857 | 2.102 |
| C-421028 | Great Slave Reef property - R190 | 749 | 149.5 | 11 | 602322 | 6734324 | Massive Ga and Sph intergrown with CCD and SD | Galena | 18.181 | 15.585 | 38.215 | 0.857 | 2.102 |
| C-421039 | Great Slave Reef property - O566 | 754 | 152.2 | 11 | 599741 | 6734164 | Coarse Ga veinlets crosscutting grey MCD; pale honey colour Sph is locally present | Galena | 18.159 | 15.580 | 38.190 | 0.858 | 2.103 |
| C-421056 | Great Slave Reef property - P499 | 744 | 91.5 | 11 | 600330 | 6733548 | Fine- to medium-grained brownish Sph forming bands and aggregates, and coarse Ga forming semi-massive bands | Galena | 18.177 | 15.603 | 38.268 | 0.858 | 2.105 |
| C-421062 | Great Slave Reef property - W19 | 219 | 141.8–143.4 | 11 | 605713 | 6735862 | Fine laces of colloform Sph and Ga crystals (<0.5 mm) in CCD | Galena | 18.189 | 15.594 | 38.228 | 0.857 | 2.102 |
| C-421221 | Windy Point property | Z29 | 49.8 | 11 | 547073 | 6790417 | Ga crystals disseminated in oil-stained whitish SD | Galena | 18.160 | 15.548 | 38.135 | 0.856 | 2.100 |
| C-421222 | Windy Point property | Z23 | 59 | 11 | 546503 | 6791087 | Disseminated Ga crystals (4–5 mm) associated with SD in vugs | Galena | 18.166 | 15.557 | 38.160 | 0.856 | 2.101 |
| C-421223 | Windy Point property | Z20 | 29.2–29.7 | 11 | 545843 | 6790747 | Clean Ga crystals associated with CCD | Galena | 18.158 | 15.544 | 38.122 | 0.856 | 2.099 |
| C-421224 | Windy Point property | Z21 | 42 | 11 | 545923 | 6790807 | Clean Ga crystals associated with CCD, SD and late calcite | Galena | 18.165 | 15.555 | 38.156 | 0.856 | 2.101 |
| C-421226 | Windy Point property | Z26 | 23.7 | 11 | 547073 | 6791947 | Clean Ga crystals | Galena | 18.159 | 15.550 | 38.138 | 0.856 | 2.100 |
| C-421228 | Qito property | Q10 | 8.2 | 11 | 559128 | 6828518 | Clean Ga crystals associated with CCD in crackle breccia | Galena | 18.166 | 15.555 | 38.160 | 0.856 | 2.101 |
| C-421229 | Qito property | Q5 | 4.2 | 11 | 557978 | 6828518 | Sph associated with SD replacing matrix dolomite and forming cement in fractures and breccias; traces of carbonate | Sphalerite | 18.684 | 15.612 | 38.551 | 0.836 | 2.063 |
| C-421230 | Hay West property | HW-80-29 | 547.7 | 11 | 520962 | 6736247 | Cg euhedral crystals of Sph (1 cm-size to several mm), 10% disseminated in white/grey sparry dolomite | Sphalerite | 18.171 | 15.563 | 38.178 | 0.856 | 2.101 |
| C-421232 | Hay West property | HW-80-15 | 642.0–647.5 | 11 | 531904 | 6722269 | Clean Ga crystals in vugs of the dolostone | Galena | 18.159 | 15.552 | 38.140 | 0.856 | 2.100 |
| C-421239 | Hay West property | HW-79-11 | 573.0–574.8 | 11 | 521206 | 6741163 | Small Sph crystals fill vugs and fractures of bioclastic/bioturb. dolostone | Sphalerite | 18.844 | 15.630 | 39.332 | 0.829 | 2.087 |
| C-421243 | Hay West property | HW-81-46 | 358.5 | 11 | 532825 | 6756291 | Clean Ga crystals associated with cg calcite in cavities and fractures | Galena | 18.159 | 15.558 | 38.165 | 0.857 | 2.102 |
| C-433001 | Top of Manetoe facies | d-50-62-20-122-15 (IOE Triad Ebbutt) | 659.0 | 10 | 530947 | 6909642 | Clean Sph crystals in SD and CCD fracture- and vein-filling cement | Sphalerite | 20.914 | 15.892 | 40.459 | 0.760 | 1.935 |

One sample, C-433001, is a mineralized dolomite at the top of the Manetoe facies. Two galena samples (C-433017 and C-433018) are from the Oldman River MVT Zn-Pb deposit in the southern Rocky Mountains.

### Results from mineralized dolomite samples

Lead isotope analyses are plotted on the "shale curve" of Godwin and Sinclair (1982), a growth curve unique to the ancient western margin of North America. On the "shale curve", the analyzed samples cluster into two distinct populations, "Cordilleran carbonate lead" and "Pine Point lead" (Fig. 11). Samples from the western Presqu'ile barrier, Peace River Arch area, Manetoe facies, and northern Rocky Mountains are highly radiogenic and fall along or on the upper extension of the "Cordilleran carbonate lead" trend (Fig. 11a). Samples from the eastern Presqu'ile barrier (i.e. Pine Point, Great Slave Reef, Hay West, Windy Point, and Qito properties), Slavey Creek, Steen River, and Zama Lake areas on the McDonald–Hay River Fault, and Jean Marie Member in the Helmet North Field of the Cordova Embayment plot within the "Pine Point lead" cluster (Fig. 11a, b).

Lead isotope values of sphalerite and galena from the mineral properties in the eastern Presqu'ile barrier (i.e. Pine Point, Great Slave Reef, Hay West, Windy Point, and Qito) plot in a tight cluster below the "shale curve", thus defining the "Pine Point lead" signature (Fig. 11a, b). Other mineralized localities along the McDonald–Hay River Fault (i.e. Slavey Creek, Steen River, and Zama Lake areas: samples 98AB3, C-406237, C-421175) and the Jean Marie Member in the Cordova Embayment (samples 7350, 7808, C-433027) also have a "Pine Point lead" signature. Only two samples from the Hay West and Qito properties plot outside the tight cluster, showing some variations in their $^{206}Pb$ values (Fig. 11a, b). The "Pine Point lead" isotopic signature in the Jean Marie Member of the Cordova Embayment was recognized in a previous study (Nelson et al., 2002) and confirmed by this study.

The lead signature belonging to the linear "Cordilleran carbonate lead" trend extends a substantial distance eastward from the Cordilleran deformation front into the Interior Platform of northeastern BC and Alberta in galena and sphalerite occurrences contained within Paleozoic carbonate beneath the Mesozoic cover (Fig. 10). Some samples from the subsurface western Presqu'ile barrier and the Peace River Arch area of the WCSB are extremely radiogenic (Fig. 11a, c). For example, lead from carbonate-hosted Zn-Pb occurrences in the Peace River Arch area falls far above the "shale curve" for common lead with radiogenic $^{206}Pb/^{204}Pb$ values of 22.3 at Oak gas field, 22.2 at Dawson oilfield, and 24.3 within the Pekisko Formation (Table 4; Fig. 11a). Lead in galena and sphalerite of carbonate deposits from the western Presqu'ile barrier and the northern Rocky Mountains are also radiogenic but they are extremely variable (Fig. 11a, b, c, d). For example, lead from sulphide deposits along the carbonate front of the western Presqu'ile barrier (samples 1426, 1245, 1904, 4818, 704, 2425) varies substantially from the least radiogenic end of the "Cordilleran carbonate lead" trend, with a $^{206}Pb/^{204}Pb$ value of 19.24 (sample 1426) to a highly radiogenic $^{206}Pb/^{204}Pb$ value of 23.71 (sample 704). Lead from these samples defines a linear array that intersects the "shale curve" at 370 Ma (Fig. 11b). Lead from the WCSB south of the Peace River Arch area, such as the Swan Hills Simonette oilfield in western Alberta, is also highly radiogenic ($^{206}Pb/^{204}Pb$ = 22.7 to 23.2; Duggan et al., 2001). Lead isotope values of galena from the Oldman River property in southern Rocky Mountains are radiogenic and plot close to the field for the northern Rocky Mountains MVT Zn-Pb deposits (Fig. 11). All these data emphasize the great variability in the isotopic composition of "Cordilleran carbonate lead", in contrast to the tight clustering of the "Pine Point lead".

## DISCUSSION AND SYNTHESIS

Hydrothermal dolomites, typified by CCD and SD, are commonly associated with sulphide mineralization in the northern Rocky Mountains MVT belt, and with carbonate-hosted petroleum reservoirs and sulphide mineralization throughout the WCSB (Machel and Mountjoy, 1986; Leach and Sangster, 1993; Davies, 1997; Nelson et al., 2002). SD and CCD have often been controversially described as "hydrothermal" (e.g. Davies, 1997; Berger and Davies, 1999; Reimer et al., 2001) and Machel and Lonnee (2002) outlined the contentions regarding the use of the term "hydrothermal dolomite" in the literature. They recognized regionally extensive bodies of hydrothermal dolomite in the northern part of the WCSB, especially north of the Peace River Arch, and as such they identified the "Presqu'ile dolomite" as being the product of regional hydrothermal fluid flow. Another example is the Manetoe saddle dolomite facies, which is interpreted as "hydrothermal-type white dolomite that formed in the subsurface at shallow depths in Late Devonian to Carboniferous time" (Morrow and Aulstead, 1995, p. 279). South of the Peace River Arch, hydrothermal dolomite is not as widespread, and it is restricted to small zones where fluids appear to have ascended via faults and fractures.

In our study, the term "hydrothermal dolomite" applies to CCD and SD that are closely associated with sulphide mineralization, situated proximal to major structures, and assumed to be the products of the interaction of high-temperature hydrothermal fluids with surrounding carbonate rocks. It follows the definition and criteria of Machel and Lonnee (2002).

Several models have been proposed for the formation of hydrothermal dolomite and associated sulphide minerals in the WCSB. The most popular one refers to fluid flow related to a combination of topographic recharge and/or tectonic compaction during either the Devonian–Mississippian Antler Orogeny or the Cretaceous–Tertiary Laramide Orogeny (Garven, 1985; Qing and Mountjoy, 1992, 1994; Machel et al., 1996; Root, 2001). A more recent model, called

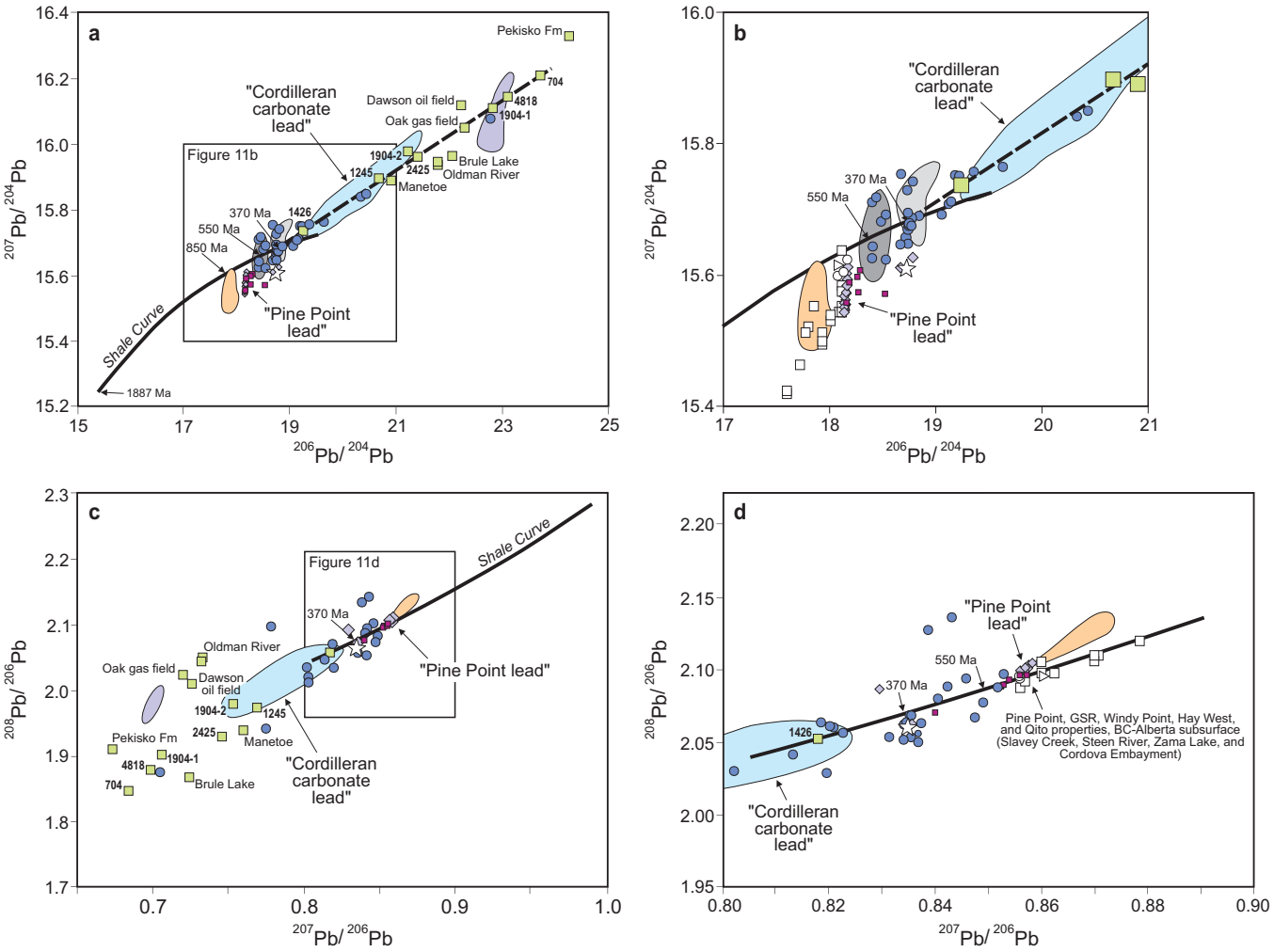


*Galena-sphalerite in Devonian carbonate of Cordova Embayment, Slavey Creek, Steen River, and Zama Lake (this study)* . . . . . ■

*Galena-sphalerite in Devonian–Mississippian carbonate of Peace River Arch, Manetoe facies, western Presqu'ile barrier, and Oldman River (this study)* . . . . . □

*Great Slave Reef, Hay West, Windy Point, Qito properties (this study), and Pine Point deposits (Cumming et al., 1990)* . . . . . ◇

*Ordovician–Devonian MVT deposits in Yukon/NWT (Godwin et al., 1982)* . . . . . ●

*Rough (Waterfall) (Godwin et al., 1982)* . . . . . ☆

*Northern Rocky Mountains MVT Pb-Zn deposits; including Manetoe facies (Godwin et al., 1982; Morrow and Cumming, 1982; Nelson et al., 2002)* . . . . . ⬭

*Swan Hills (Duggan et al., 2001)* . . . . . ⬭

Devonian–Mississippian deposits, Europe and North America

*MVT deposits from the Cornwallis Fold Belt, Nunavut (Heal, 1976)* . . . . ⬭

*Iberian Pyrite Belt (Marcoux, 1998)* . . . . . ▷

*Navan deposit (Mills et al., 1987)* . . . . . □

*Rammelsberg, Meggen deposits (Wedepohl et al., 1978)* . . . . . ○

*Syngenetic Cambrian SEDEX occurrences, Canadian Cordillera (Godwin and Sinclair, 1982)* . . . . . ⬭

*Syngenetic Upper Devonian SEDEX occurrences, Canadian Cordillera (Godwin and Sinclair, 1982)* . . . . . ⬭

**Figure 11.** Lead isotopic data from western Canadian MVT Zn-Pb deposits and carbonate-hosted sphalerite and galena occurrences in the Western Canada Sedimentary Basin and the northern Rocky Mountains. **a.** $^{207}Pb/^{204}Pb$ vs. $^{206}Pb/^{204}Pb$. **b.** Blowup of $^{207}Pb/^{204}Pb$ vs. $^{206}Pb/^{204}Pb$. **c.** $^{208}Pb/^{206}Pb$ vs. $^{207}Pb/^{206}Pb$. **d.** Blowup of $^{208}Pb/^{206}Pb$ vs. $^{207}Pb/^{206}Pb$. These plots include new data from subsurface occurrences (see Table 4 for data and Fig. 10 for location of samples) and data from the literature (see legend). Devonian–Mississippian syngenetic/diagenetic massive sulphide deposits from Europe and North America are shown for comparison with the Pine Point deposits.

hydrothermal convection, infers that CDD, SD, and associated sulphide minerals in the WCSB (north of the Peace River Arch) and the northern Rocky Mountains MVT belt formed during Devonian–Mississippian tectonic activity on the western margin of North America (Paradis and Nelson, 2000; Nelson et al., 2002). High heat flow and the development of deep hydrothermal convection systems were generated in an actively rifting back-arc setting eastward of an easterly dipping subduction zone that evolved along the western continental margin in early Devonian time. The subduction and rollback of the slab created arc and back-arc volcanic--plutonic-sedimentary complexes in the Canadian Cordillera. These arc and back-arc systems were affected by episodic rifting, which generated hydrothermal activity and formation of volcanic-hosted massive sulphide (VHMS) deposits in the outermost continental margin (i.e. the pericratonic terranes), sedimentary exhalative (SEDEX) deposits in a more inland belt of continent-margin basins (i.e. Kechika Trough and Selwyn Basin), and Mississippi Valley-type (MVT) deposits on the continental platform. The carbonate-hosted Zn-Pb mineralization and hydrothermal dolomite of the Rocky Mountains and the WCSB (north of the Peace River Arch) are products of this far-reaching subduction effect and genesis of hydrothermal activity resulting in fluids being driven along reactivated back-arc structures, faults, and permeable strata. Goodfellow et al. (1993) also argued for a connection between northern Cordilleran SEDEX and MVT deposits, based on the spatial association of MVT deposits with the rifted margins of anoxic basins, the similarity of metal ratios, and the similar heavy and variable sulphur isotope values. They envisaged a mixing model, in which reduced and sulphur-bearing fluids circulating in porous and permeable carbonate rocks encountered metal-bearing fluids rising along basement structures to the site of ore deposition. The McDonald–Hay River Fault and other northeast-trending faults, such as the Rabbit Lake Fault Zone and the Hay River Fault Zone, are likely candidates for this role of providing conduits for basement-derived metal-bearing fluids.

The case for a Devonian–Mississippian age for the carbonate-hosted Zn-Pb mineralization and hydrothermal dolomite of the northern Rocky Mountains and WCSB was discussed by Nelson et al. (2002). Therefore, assuming that MVT Zn-Pb mineralization and hydrothermal dolomite are coeval and syngenetic, we first discuss their isotopic linkages and trends, and then discuss the results in terms of fluid flow and mineralizing systems.

## Carbon, oxygen, strontium isotope signatures and linkages

Mineralized and nonmineralized CCD and SD at any given locality within the eastern Presqu'ile barrier, western Presqu'ile barrier, northern Rocky Mountains and Mackenzie Mountains have similar C, O, and Sr isotopic signatures (Fig. 7). Only $^{86}Sr/^{87}Sr$ values from the Robb Lake deposit are higher than most values for the eastern and western Presqu'ile barrier and areas along the McDonald–Hay River Fault. They are also higher than the 0.7120 value of MASIRBAS. This indicates that "radiogenic" strontium (i.e. $^{87}Sr$) was preferentially introduced into the carbonate deposits at Robb Lake during dolomitization and mineralization. Solutions with strontium isotope ratios in excess of 0.7100 can develop through the interaction of deeply circulating fluids with fine-grained siliciclastic rocks (Morrow et al., 1990), which contain alkali feldspars rich in radiogenic strontium.

The similarity in isotopic signatures suggests a link between sulphide mineralization and hydrothermal dolomitization. It also implies the composition of fluids responsible for dolomitization and mineralization was similar in terms of C and O isotopes, as well as Sr isotopes to some extent.

## Isotopic trends

The isotopic data illustrate a broad westward decrease in $\delta^{18}O$ values and increase in $^{87}Sr/^{86}Sr$ ratios of mineralized CCD and SD from the eastern Presqu'ile barrier to the Rocky and Mackenzie Mountains (Fig. 8a, c). The nonmineralized dolomite samples do not show a westward decrease in $\delta^{18}O$ values since the range of values for the Manetoe facies overlaps those of the eastern and western Presqu'ile barrier. However, these dolomite samples do show a broad increase in $^{87}Sr/^{86}Sr$ ratios from the eastern Presqu'ile barrier to the Rocky and Mackenzie mountains.

Qing and Mountjoy (1994) observed a regional trend of gradually decreasing $\delta^{18}O$ values and increasing $^{86}Sr/^{87}Sr$ ratios westward from the Pine Point deposits to northeastern BC in dolomite of the Presqu'ile barrier. They attributed the trend of decreasing $\delta^{18}O$ values to a westerly increase in fluid inclusion $Th_L$ from 92° to 121°C at Pine Point to 139° to 178°C in the western Presqu'ile barrier. Turner (2006) also observed an increase of $Th_L$ in sphalerite from Pine Point (53–67°C; ave. = 61°C ± 4.9 [1σ], n=7) to the Great Slave Reef property (62–112°C; ave. = 97°C ± 13.6 [1σ], n=16), and also a small increase of $Th_L$ in SD from Pine Point (85–93°C; ave. = 89°C ± 2.7 [1σ], n=10) to the Windy Point property (96–125°C; ave. = 106°C ± 8.8 [1σ], n=14). Turner (2006) did not analyze samples in the western Presqu'ile barrier. Surprisingly, given the western location of Robb Lake in the Rocky Mountains with exceptionally low $\delta^{18}O$ values (-15.6 to -13.8), its primary and pseudosecondary fluid inclusions show only moderately elevated $Th_L$ of 87 to 154°C, averaging 119°C (Sangster and Carrière, 1991). These moderate and variable fluid temperatures are intriguing and unexplained at the moment. Low $^{18}O$ values of –18.4 to –17.3‰ and fluid inclusion $Th_L$ of 138 to 152°C were also found in dolomite cements of the Cathedral Formation in the southern Canadian Rocky Mountains (Yang et al., 1995). Yang et al. (1995) interpreted the negative $\delta^{18}O$ values to elevated temperatures of dolomitization.

Low $\delta^{18}O$ values along with high $^{87}Sr/^{86}Sr$ ratios within and proximal to the Rocky Mountains can be ascribed, respectively, to high-temperature fluids and the influence of siliciclastic sources. Although such fluids are often linked to deep sedimentary and tectonic burial during the Late Devonian to Early Carboniferous Antler Orogeny or the Late Jurassic to Early Tertiary Laramide Orogeny, they could also have arisen as hydrothermal solutions channelled along intrabasinal faults. Morrow (1998) explained the westward-decreasing trend in $\delta^{18}O$ values as being a function of long-lived, deep convective circulation of hydrothermal fluids to great depths relative to the Precambrian basement in late Paleozoic time.

The sudden eastward decrease in $^{87}Sr/^{86}Sr$ ratios near the Cordilleran limit of deformation suggests that fluids interacted with siliciclastic rocks or underlying Precambrian basement in the zone of deformation and became rapidly less radiogenic as they migrated eastward through the Presqu'ile barrier or the McDonald–Hay River Fault system. This reduction in the radioactive $^{87}Sr$ isotope could be due to dilution by less radiogenic formation waters at shallower depths in the Presqu'ile barrier, incorporation of less radiogenic Sr from non-radiogenic Middle Devonian limestone, or mixing with fluids from a different source (Mountjoy et al., 1992). All mineralized carbonate samples from the Rocky Mountains have $^{87}Sr/^{86}Sr$ values greater than 0.7100, indicating a significant input of radiogenic strontium to the mineralizing fluids. Their strontium ratios are similar to those of the SEDEX deposits of the Selwyn Basin, which have values of 0.7129 to 0.7144 for barite at Jason (Turner et al., 1989), and 0.7140 to 0.7170 for carbonate samples at Howards Pass (Goodfellow and Jonasson, 1984). Samples with $^{87}Sr/^{86}Sr$ values greater than 0.7120 (e.g. MASIRBAS) fall within Machel and Cavell's (1999) field for cements generated by extrabasinal fluids; that is, fluids that have interacted with Precambrian siliciclastic rocks. Unlike Sr-isotopic compositions of carbonate rocks farther east along the Presqu'ile barrier, those from the northern Rocky Mountains, such as Robb Lake (0.7118–0.7178) and to some extent the Manetoe facies (0.71123–0.71156), and those from the southern Rocky Mountains, such as Oldman River (0.71034–0.71044) and Monarch-Kicking Horse and Mount Brussilof (0.7090–0.7120; Nesbitt and Muehlenbachs, 1994), suggest that dolomitizing and mineralizing fluids reflect fluid sources that interacted with continental siliciclastic rocks.

## Lead isotope regional signatures

Two distinct types of metal dispersal systems were operative in the northern Canadian Rocky Mountains and the WCSB, and gave rise to two lead populations: the "Cordilleran carbonate lead" trend and the "Pine Point lead" cluster.

The "Cordilleran carbonate lead" trend, which is characteristic of the northern Rocky Mountains MVT belt, extends east into the western Presqu'ile barrier and the Peace River Arch area of the WCSB (Fig. 10). It is also present in the Swan Hill Formation buildups of the Simonette oilfield of west-central Alberta (Duggan et al., 2001). It forms a linear trend that intersects the "shale growth curve" in the Devonian–Mississippian range (370 Ma) (Fig. 11b, d). This intersection is also defined by a cluster of analyses (Fig. 11b) from Ordovician–Devonian MVT deposits of the Mackenzie Mountains (Godwin et al., 1982), and one from the Rough (Waterfall) carbonate-hosted deposit within the Kechika Trough (Godwin and Sinclair, 1982). These signatures also overlap the field for Devonian SEDEX deposits of the Selwyn Basin and Kechika Trough (Fig. 11b).

The "Cordilleran carbonate lead" trend is consistent with northeasterly fluid flow paths from the miogeocline into the Devonian carbonate aquifers of the WCSB. It is similar to the lead isotopic trends shown by classic MVT deposits of the central United States, which are interpreted as mixing lines between ordinary upper crustal lead and an anomalous lead that is far more radiogenic than any known average crustal source (Heyl et al., 1974). Many authors have advocated regional fluid flow in sandstone aquifers as the source of lead in carbonate-hosted deposits (cf. Goldhaber et al., 1995). Others have suggested the underlying Precambrian basement as the source for lead. With decreasing fluid temperatures eastward away from the Rocky Mountain front, the fluids may have become more enriched in radiogenic lead as a result of preferential extraction of radiogenic lead from metamict zircons rather than equilibrium extraction of combined radiogenic and common leads from feldspars (cf. Nelson et al., 2002). The "Cordilleran carbonate lead" trend, therefore, appears to define a mixing line between the "least" radiogenic values represented by the Devonian SEDEX deposits and an extremely radiogenic end-member of unknown origin, and results from a non-equilibrium process of lead extraction.

In marked contrast to the highly elongate, linear "Cordilleran carbonate lead" trend, the "Pine Point lead" forms a tight cluster that plots close to the Early Cambrian range on the "shale curve", nearly 200 Ma older than their host rocks (Fig. 11b). This suggests that the source of lead for Pine Point was much less radiogenic than that of the Cordilleran SEDEX deposits, and that it was unrelated to that of the Cordilleran miogeocline. The fields for Cambrian and Devonian SEDEX deposits have been plotted on Figure 11 to show how distinctive the Pine Point cluster is compared to SEDEX deposits of the Canadian Cordillera. In fact, it plots within a well-constrained field along with other Devonian–Mississippian SEDEX and MVT deposits of continental to pericratonic settings, such as Rammelsberg/Meggen, Navan, and the Iberian Pyrite belt, and is slightly more radiogenic than leads from the Late Devonian Cornwallis Fold Belt (Nelson et al., 2002). Nelson et al. (2002) interpreted the "Pine Point lead" as a typical signature for Devonian–Mississippian northern hemisphere continental leads.

The location of the Pine Point, Great Slave Reef, Hay West, Windy Point, and Qito deposits along the McDonald–Hay River Fault and other subparallel northeast-trending

faults may account for their lead isotopic signature. Geological and isotopic evidence points to a key role for the fault systems in the formation of orebodies within the Pine Point district (Rhodes et al., 1984). Krebs and Macqueen (1984) suggested that the origin of the orebodies was linked to fluid expulsion along the fault systems. Others suggested that there is a sub-regional structural control on the distribution of orebodies within the Pine Point district by a local set of east-west faults extending westward from the McDonald–Hay River Fault to Pine Point (e.g. Skall, 1975). The role of the faults and the structural control on ore deposition also explain the "Pine Point lead" signature of samples collected along the McDonald–Hay River Fault at Zama Lake, Steen River, and Slavey Creek. Structural control could also explain the "Pine Point lead" signature found in the Jean Marie Member in the Helmet North gas field of the Cordova Embayment, which lies along the trace of northeast-trending faults that exist between the Hay River Fault Zone and the McDonald–Hay River Fault (Morrow et al., 2006). Several faults in this area coincide with an apparent dextral offset of basement domains (Morrow et al., 2006), and some of them show 50 to 70 m pre-Devonian throws (J. Wendte, pers. comm., 1998). Other deposits in the world such as those of the Tri-State MVT Zn-Pb district in central United States, the Alpine district in Europe, and the Lennard Shelf MVT district in western Australia are structurally controlled, and there is a growing recognition among geologists that fluid movements responsible for MVT mineralization tend to be focused along faults (Keller et al., 2000).

We speculate that the source of the "Pine Point lead" was leached directly from rocks of the Precambrian basement by fluids circulating in deep fault structures, such as the McDonald–Hay River Fault and other northeast-trending faults (e.g. Rabbit Lake Fault Zone and the Hay River Fault Zone). Lithogeochemical and isotopic analyses of metal-bearing basement rocks in the region need to be completed before further inferences can be made.

### Regional paleofluid flow

The data from this study place some constraints on the paleofluid flow and mineralizing systems within the northern Rocky Mountains MVT belt and the WCSB, north of the Peace River Arch. The oxygen, carbon, and strontium isotopes and fluid inclusion data support a link between MVT carbonate-hosted Zn-Pb mineralization and hydrothermal dolomitization within the northern Canadian Rocky Mountains and the Western Canada Sedimentary Basin (WCSB). Coprecipitation of CCD, SD, and sulphides, and similar isotopic signature between mineralized and nonmineralized CCD and SD implies similar parent fluids. Isotopic trends support easterly formation fluid-flow paths from the Rocky Mountains into the western continental platform and indicate a key role for the northeast-trending structures, such as the McDonald–Hay River Fault, Rabbit Lake Fault Zone, Hay River Fault Zone, and the Presqu'ile barrier, in the circulation of hydrothermal fluids as well as mineralizing processes. The lead isotope data favour two distinct types of metal dispersal systems in the northern Rockies and the WCSB: 1) A widespread, radiogenic "Cordilleran carbonate lead" characteristic of the northern Rocky Mountains MVT belt extending eastward into the WCSB, and 2) a more localized, nonradiogenic "Pine Point lead", characteristic of the eastern Presqu'ile barrier and areas along the McDonald–Hay River Fault system. Lead isotope data suggest that deep fluid circulation through Precambrian basement rocks beneath the McDonald–Hay River Fault provided the source of metals for the Pine Point deposits and other mineralized areas along the fault. Other northeast-trending faults parallel to the McDonald–Hay River Fault may also have played a role in mineralizing carbonate occurrences along the Presqu'ile barrier, west of Pine Point.

In terms of exploration potential, this makes the areas along the McDonald–Hay River Fault and the Devonian carbonate rocks of the Cordova Bay Embayment excellent targets for significant MVT Zn-Pb deposits.

## CONCLUSIONS

Hydrothermal dolomite (i.e. coarse-crystalline dolomite and saddle dolomite) associated with sulphide mineralization at Great Slave Reef, Hay West, Windy Point, and Qito properties within the eastern Presqu'ile barrier have $\delta^{18}O$, $\delta^{13}C$ and $^{87}Sr/^{86}Sr$ values similar to published values for nonmineralized dolomite samples from the eastern Presqu'ile barrier. Mineralized dolomite of the Robb Lake deposit and Manetoe facies in the Rocky and Mackenzie Mountains have similar $\delta^{18}O$ and $\delta^{13}C$ values to those from the western Presqu'ile barrier, but their $^{87}Sr/^{86}Sr$ values are more radiogenic than most dolomite rocks of the western and eastern Presqu'ile barrier and the interior of the WCSB. This suggests that siliciclastic rocks or the Precambrian basement influenced the composition of the mineralizing fluids.

A westward decrease in $\delta\ ^{18}O$ values and increase in $^{87}Sr/^{86}Sr$ ratios is observed in mineralized dolomite from the eastern Presqu'ile barrier to the Rocky and Mackenzie mountains. The nonmineralized dolomite does not show a westward trend in $\delta\ ^{18}O$ values, but does show a broad increase in $^{87}Sr/^{86}Sr$ ratios from the eastern Presqu'ile barrier to the Rocky and Mackenzie mountains. $^{87}Sr/^{86}Sr$ values also increase westward along the McDonald–Hay River Fault from Pine Point to the Robb Lake deposit in the Rocky Mountains. This points to easterly fluid-flow paths from the Rocky Mountains to the western continental platform, and a key role for the McDonald–Hay River Fault and other northeast-trending structures, such as the Rabbit Lake Fault Zone, the Hay River Fault Zone, and the Presqu'ile barrier, in the circulation of hydrothermal fluids and mineralizing processes.

Two distinct lead isotopic signatures characterize the sulphide minerals associated with carbonate deposits in the northern Rocky Mountains MVT belt and the WCSB. A linear, highly radiogenic lead isotopic signature is characteristic of the northern Rocky Mountains MVT belt, the Manetoe facies, the western Presqu'ile barrier, and the Peace River Arch area of the WCSB. By contrast, subsurface samples from the Great Slave Reef, Hay West, Windy Point, and Qito properties, and several subsurface samples from directly above the McDonald–Hay River Fault, have uniform, non-radiogenic values, identical to the Pine Point cluster. These two strongly contrasting lead isotopic populations suggest that two, separate, metal-bearing fluid sources/pathways existed in the WCSB. The "Cordilleran carbonate lead" with a widespread distribution in the Rocky Mountains and the WCSB (except for the northeast-trending faults and areas around Pine Point) involved non-equilibrium lead extraction from Precambrian basement rocks or sandstone aquifers, and enrichment in radiogenic lead with decreasing fluid temperature away from the Rocky Mountain front. The "Pine Point lead" involved deep, metal-bearing fluid circulation along the McDonald–Hay River Fault and other northeast-trending faults parallel to the McDonald–Hay River Fault. The local Precambrian basement rocks were probably the sources of metals for the Pine Point district and mineralizing sites along the McDonald–Hay River Fault. Lithogeochemical and isotopic analyses of sulphide-bearing basement rocks need to be completed however, to confirm this hypothesis.

## ACKNOWLEDGMENTS

This study was done under the auspices of the Targeted Geoscience Initiative (TGI) "Potential for carbonate-hosted Zn-Pb (MVT) deposits in northern Alberta and southern Northwest Territories", which was a collaborative project between the Geological Survey of Canada, the C.S. Lord Northern Geoscience Centre, and the Alberta Geological Survey.

We are extremely grateful to R. Eccles who helped us in the selection of the samples for isotopic analyses. We are grateful to Peter Hannigan for critical reading of the manuscript and providing constructive comments. We also thank Guoxiang Chi for his thorough review. We are most grateful to Rob Creaser and Janet Gabites for strontium and lead isotope analyses. Several figures were drafted by Richard Franklin of the Geological Survey of Canada, Pacific Division.

## REFERENCES

**Adams, J.J., Rostron, B.J., and Mendoza, C.A.**
2000: Evidence for two-fluid mixing at Pine Point, NWT; Journal of Geochemical Exploration, v. 69–70, p. 103–108.

**Al-Aasm, I.**
2003: Origin and characterization of hydrothermal dolomite in the Western Canada Sedimentary Basin; Journal of Geochemical Exploration, v. 78–79, p. 9–15.

**Amthor, J.E., Mountjoy, E.W., and Machel, H.G.**
1993: Subsurface dolomites in the Upper Devonian Leduc Formation buildups, central part of the Rimbey-Meadowbrook trend, Alberta, Canada; Bulletin of Canadian Petroleum Geology, v. 41, p. 164–185.

**Berger, Z. and Davies, G.**
1999: The development of linear hydrothermal dolomite (HTD) reservoir facies along wrench or strike slip fault systems in the Western Canada Sedimentary Basin; Canadian Society of Petroleum Geologists, Reservoir, v. 26, no. 1, p. 34–38.

**Bodnar, R.J. and Vityk, M.O.**
1994: Interpretation of microthermometric data for $H_2O$-NaCl fluid inclusions; *in* Fluid inclusions in minerals: Methods and Applications, (ed.) B. De Vivo and M.L. Frezzotti; Virginia Tech, Blacksburg, VA, p. 117–130.

**Coniglio, M., Morrow, D.W., and Wilson, N.**
2006: Reassessment of Middle Devonian dolomite, Presqu'ile barrier, Northwest Territories; *in* Potential for Carbonate-hosted Lead-zinc Mississippi Valley-type Mineralization in Northern Alberta and Southern Northwest Territories: Geoscience Contributions, Targeted Geoscience Initiative, (ed.) P.K. Hannigan; Geological Survey of Canada, Bulletin 591.

**Craig, H.**
1957: Isotopic standards for carbon and oxygen and correction factors for mass spectrometric analysis of carbon dioxide; Geochimica et Cosmochimica Acta, v. 12, no. 1-2, p. 133–149.

**Cumming, G.L., Kyle, J.R., and Sangster, D.F.**
1990: Pine Point: A case history of lead isotopic homogeneity in a Mississippi Valley-type district; Economic Geology, v. 85, p. 133–144.

**Davies, G.R.**
1997: Hydrothermal dolomite (HTD) reservoir facies: Global perspectives on tectonic-structural and temporal linkage between MVT and SEDEX Pb-Zn ore bodies, and subsurface HTD reservoir facies; Canadian Society of Petroleum Geologists, Short Course Notes, Graham Davies Geological Consultants, 167 p.

**Douglas, R.J.W., Gabrielse, H., Wheeler, J.O., Stott, D.F., and Belyea, H.R.**
1970: Geology of western Canada; *in* Geology and Economic Minerals of Canada; Geological Survey of Canada, Economic Geology Report no. 1, p. 366–488.

**Duggan, J.P., Mountjoy, E.W., and Stasiuk, L.D.**
2001: Fault-controlled dolomization at Swan Hills Simonette oil field (Devonian), deep basin west-central Alberta, Canada; Sedimentology, v. 48, p. 301–323.

**Ferri, F., Rees, C., Nelson, J., Legun, A., Orchard, M.J., Norford, B.S., Fritz, W.H., Mortensen, J.K., and Gabites, J.E.**
1999: Geology and mineral deposits of the northern Kechika Trough between Gataga River and the 60$^{th}$ parallel; British Columbia Ministry of Energy and Mines, Bulletin 107, 122 p.

**Friedman, I. and O'Neil, J.R.**
1977: Compilation of stable isotope fractionation factors of geochemical interest; *in* Data of Geochemistry, (ed.) M. Fleischer, Chapter KK; U.S. Geological Survey Professional Paper 440-KK, 12 p.

**Fritz, P. and Jackson, S.A.**
1972: Geochemical and isotopic characteristics of Middle Devonian dolomites from Pine Point, northern Canada; 24th International Geological Congress, Montreal, Proceedings, Section 6, Stratigraphy and Sedimentology, p. 230–243.

**Garven, G.**
1985: The role of regional fluid flow in the genesis of the Pine Point deposit, Western Canada Sedimentary Basin; Economic Geology, v. 80, p. 307–324.

**Godwin, C.J. and Sinclair, A.J.**
1982: Average lead isotope growth curves for shale-hosted zinc-lead deposits, Canadian Cordillera; Economic Geology, v. 77, p. 675–690.

**Godwin, C.J., Sinclair, A.J., and Ryan, B.D.**
1982: Lead isotope models for the genesis of carbonate-hosted Zn-Pb, shale-hosted Ba-Zn-Pb, and silver-rich deposits in the northern Canadian Cordillera; Economic Geology, v. 77, p. 82–94.

**Goldhaber, M.B., Church, S.E., Doe, B.R., Aleinikoff, J.N., Brannon, J.C., Podosek, F.A., Mosier, E.L., Taylor, C.D., and Gent, C.A.**
1995: Lead and sulfur isotope investigation of Paleozoic sedimentary rocks from the southern Midcontinent of the United States; implications for paleohydrology and ore genesis of the Southeast Missouri lead belts; Economic Geology, v. 90, no. 7, p. 1875–1910.

**Goodfellow, W.D. and Jonasson, I.R.**
1984: Ocean stagnation and ventilation defined by $\delta^{34}S$ secular trends in pyrite and barite, Selwyn Basin, Yukon; Geology, v. 12, no. 10, p. 583–586.

**Goodfellow, W.D., Lydon, J.W., and Turner, R.J.W.**
1993: Geology and genesis of stratiform sediment-hosted (SEDEX) zinc-lead-silver sulfide deposits; *in* Mineral Deposit Modelling, (ed.) R.V. Kirkham, W.D. Sinclair, R.I. Thorpe and J.M. Duke; Geological Association of Canada, Special Paper 40, p. 201–251.

**Heal, G.E.N.**
1976: The Wrigley-Lou and Polaris-Truro lead-zinc deposits, Northwest Territories; M.Sc. thesis, University of Alberta, 172 p.

**Heyl, A.V., Landis, G.P., and Zartman, R.E.**
1974: Isotopic evidence for the origin of Mississippi Valley-type mineral deposits: A review; Economic Geology, v. 69, p. 992–1006.

**Hoffman, P.F.**
1987: Continental transform tectonics; Great Slave Lake shear zone (ca. 1.9 Ga), northwest Canada; Geology, v. 15, no. 9, p. 785–788.

**Hurley, N.F. and Lohmann, K.C.**
1989: Diagenesis of Devonian reefal carbonates in the Oscar Range, Canning Basin, Western Australia; Journal of Sedimentary Petrology, v. 59, no. 1, p. 127–145.

**Keller, T.J., Gregg, J.M., and Shelton, K.L.**
2000: Fluid migration and associated diagenesis in the greater Reelfoot Rift region, Midcontinent, United States; Geological Society of America, Bulletin, v. 112, no. 11, p. 1680–1693.

**Krebs, W. and Macqueen, R.**
1984: Sequence of diagenetic and mineralization events, Pine Point lead-zinc property, Northwest Territories, Canada; Bulletin of Canadian Petroleum Geology, v. 32, no. 4, p. 434–464.

**Kyle, J.R.**
1977: Development of sulphide hosting structures and mineralization, Pine Point, Northwest Territories; Ph.D. thesis, University of Western Ontario, 226 p.
1981: Geology of the Pine Point lead-zinc district; *in* Handbook of Strata-Bound and Stratiform Ore Deposits, (ed.) K.H. Wolf; Elsevier Publishing Co., Amsterdam, Netherlands, Part III, v. 9, p. 643–741.

**Leach, D.L. and Sangster, D.F.**
1993: Mississippi Valley-type lead-zinc deposits; *in* Mineral Deposit Modelling, R.V. Kirkham, (ed.) W.D. Sinclair, R.I. Thorpe, and J.M. Duke; Geological Association of Canada, Special Paper 40, p. 289–314.

**Lonnee, J. and Al-Aasm, I.S.**
2000: Dolomitization and fluid evolution in the Middle Devonian Sulphur Point Formation, Rainbow South Field, Alberta: Petrographic and geochemical evidence; Bulletin of Canadian Petroleum Geology, v. 48, no. 3, p. 262–283.

**Machel, H.G. and Cavell, P.A.**
1999: Low-flux, tectonically-induced squeegee fluid flow ("hot flash") into the Rocky Mountain foreland basin; Bulletin of Canadian Petroleum Geology, v. 47, no. 4, p. 510–533.

**Machel, H.G. and Lonnee, J.**
2002: Hydrothermal dolomite – a product of poor definition and imagination; Sedimentary Geology, v. 152, p. 163–171.

**Machel, H.G. and Mountjoy, E.W.**
1986: Chemistry and environments of dolomitization – a reappraisal. Earth- Science Reviews, v. 23, no. 3, p. 175–222.

**Machel, H.G., Cavell, P.A., and Patey, K.S.**
1996: Isotopic evidence for carbonate cementation and recrystallization, and for tectonic expulsion of fluids into the Western Canada Sedimentary Basin; Geological Society of America, Bulletin, v. 108, no. 9, p. 1108–1119.

**Marcoux, E.**
1998: Lead isotopic systematics of the giant massive sulphide deposits in the Iberian Pyrite Belt; Mineralium Deposita, v. 33, no. 1-2, p. 45–58.

**McClay, K.R., Insley, M.W., and Anderton, R.**
1989: Inversion of the Kechika Trough, northeastern British Columbia, Canada; *in* Inversion Tectonics Meeting, (ed.) M.A. Cooper and G.D. Williams; Geological Society of London, Special Publication 44, p. 235–257.

**McCrea, J.M.**
1950: On the isotopic chemistry of carbonates and a paleothermometer scale; Journal of Chemical Physics, v. 18, p. 849–857.

**Mills, H., Halliday, A.N., Ashton, J.H., Anderson, I.K., and Russell, M.J.**
1987: Origin of a giant orebody at Navan, Ireland; Nature, v. 327, no. 6119, p. 223–226.

**Morrow, D.W.**
1998: Regional subsurface dolomitization: Models and constraints; Geoscience Canada, v. 25, no. 2, p. 57–70.

**Morrow, D.W. and Aulstead, K.L.**
1995: The Manetoe Dolomite – a Cretaceous-Tertiary or a Paleozoic event? Fluid inclusion and isotopic evidence; Bulletin of Canadian Petroleum Geology, v.43, no. 3, p. 267–280.

**Morrow, D.W. and Cumming, G.L.**
1982: Interpretation of lead isotope data from zinc-lead mineralization in the northern part of the western Canadian Cordillera; Canadian Journal of Earth Sciences, v. 19, p. 1070–1078.

**Morrow, D.W., Cumming, G.L., and Aulstead, K.L.**
1990: The gas-bearing Devonian Manetoe facies, Yukon and Northwest Territories; Geological Survey of Canada, Bulletin 400, 54 p.

**Morrow, D.W., MacLean, B.C., Miles, W.F., Tzeng, P., and Pană, D.**
2006: Subsurface structures in southern Northwest Territories and northern Alberta: Implications for mineral and petroleum potential; *in* Potential for Carbonate-hosted Lead-zinc Mississippi Valley-type Mineralization in Northern Alberta and Southern Northwest Territories: Geoscience Contributions, Targeted Geoscience Initiative, (ed.) P.K. Hannigan; Geological Survey of Canada, Bulletin 591.

**Mossop, G. and Shetsen, I. (compilers)**
1994: Geological Atlas of the Western Canada Sedimentary Basin; Calgary, Canadian Society of Petroleum Geologists and Alberta Research Council, 510 p.

**Mountjoy, E.W., Qing, H., and MacNutt, R.H.**
1992: Strontium isotopic composition of Devonian dolomites, Western Canada Sedimentary Basin: Significance of sources of dolomitizing fluids; Applied Geochemistry, v. 7, p. 59–75.

**Mountjoy, E.W., Machel, H.G., Green, D., Duggan, J., and Williams-Jones, A.E.**
1999: Devonian matrix dolomites and deep burial carbonate cements: A comparison between the Rimbey-Meadowbrook reef trend and the deep basin of west-central Alberta; Bulletin of Canadian Petroleum Geology, v. 47, no. 4, p. 487–509.

**Nelson, J., Paradis, S., Christensen, J., and Gabites, J.**
2002: Canadian Cordilleran Mississippi Valley-type deposits: A case for Devonian-Mississippian back-arc hydrothermal origin; Economic Geology, v. 97, p. 1013–1036.

**Nesbitt, B.E. and Muehlenbachs, K.**
1994: Paleohydrology of the Canadian Rockies and origins of brines, Pb-Zn deposits and dolomitization in the Western Canada Sedimentary Basin; Geology, v. 22, p. 243–246.

**Norris, A.W.**
1965: Stratigraphy of Middle Devonian and older Palaeozoic rocks of the Great Slave Lake region, Northwest Territories; Geological Survey of Canada, Memoir 322, 180 p.

**Oakes, C.S., Bodnar, R.J., and Simonson, J.M.**
1990: The system NaCl-$CaCl_2$-$H_2O$: I. The ice liquidus at 1 atm total pressure; Geochimica et Cosmochimica Acta, v. 54, no. 3, p. 603–610.

**Oakes, C.S., Sheets, R.W., and Bodnar, R.J.**
1992: (NaCl+$CaCl_2$){aq}: Phase equilibria and volumetric properties (extended abstract); *in* Fourth Biennial Pan-American Conference on Research in Fluid Inclusions; Program and Abstracts, p. 128–132.

**Olson, R.A., Dufresne, M.B., Freeman, M.E., Eccles, D.R., and Richardson, R.J.H.**
1994: Regional metallogenic evaluation of Alberta; Alberta Geological Survey Open File Report 1994-8, 50 p.

**Paradis, S. and Nelson, J.L.**
2000: The Devonian-Mississippian metallogenetic history of Western Canada, from leading plate margin to continent interior; Abstract and oral presentation at "Volcanic Environments and Massive Sulphide Deposits", Program with Abstracts, CODES (Centre for Ore Deposit Research), Tasmania, Australia, November 2000.

**Paradis, S., Nelson, J.L., and Irwin, S.E.**
1998: Age constraints on the Devonian shale-hosted Zn-Pb-Ba deposits, Gataga District, northeastern British Columbia, Canada; Economic Geology, v. 93, p. 184–200.

**Qing, H.**
1986: Diagenesis and sedimentology of Rainbow F and E buildups (Middle Devonian), northwestern Alberta; MSc thesis, McGill University, Montreal, 150 p.
1991: Diagenesis of Middle Devonian Presqu'ile dolomite Pine Point NWT and adjacent subsurface; Ph.D. thesis, McGill University, Montreal, 292 p.

**Qing, H. and Mountjoy, E.W.**
1992: Large-scale fluid-flow in the Middle Devonian Presqu'ile barrier, Western Canada Sedimentary Basin; Geology, v. 20, p. 903–906.
1994: Formation of coarsely crystalline, hydrothermal dolomite reservoirs in the Presqu'ile Barrier, Western Canada Sedimentary Basin; American Association of Petroleum Geologists, Bulletin, v. 78, no. 1, p. 55–77.
1995: Paleohydrogeology of the Canadian Rockies and origins of brines, Pb-Zn deposits and dolomitization in the Western Canada Sedimentary Basin: Comment; Geology, v. 23, p. 189–190.

**Randall, A.W., Barr, D.A., and Giroux, G.H.**
1986: Geological aspects of ore reserve estimates, Pine Point District zinc-lead deposits, N.W.T.; *in* Applied Mining Geology; Ore Reserve Estimation, (ed.) D.E. Ranta; Society of Mining Engineers of AIME, p. 175–197.

**Reimer, J.D., Hudema, T., and Viau, C.**
2001: TSR-HTD ten years later: an exploration update, with examples from western and eastern Canada; Canadian Society of Petroleum Geologists Annual Convention Abstracts, p. 276–279.

**Rhodes, D., Lantos, E.A., Lantos, J.A., Webb, R.J., and Owens, D.C.**
1984: Pine Point ore bodies and their relationship to the stratigraphy, structure, dolomitization and karstification of the Middle Devonian barrier complex; Economic Geology, v. 79, p. 991–1055.

**Roedder, E.**
1968: Temperature, salinity, and origin of the ore-forming fluids at Pine Point, Northwest Territories, Canada, from fluid inclusion studies; Economic Geology, v. 63, no. 5, p. 439–450.

**Root, K.G.**
2001: Devonian Antler fold and thrust belt and foreland basin development in the southern Canadian Cordillera: implications for the Western Canada Sedimentary Basin; Bulletin of Canadian Petroleum Geology, v. 49, no. 1, p. 7–36.

**Ross, G., Parrish, R.R., Villeneuve, M.E., and Bowring, S.A.**
1991: Geophysics and geochronology of the crystalline basement of the Alberta Basin, western Canada; Canadian Journal of Earth Sciences, v. 28, no. 4, p. 512–522.

**Sangster, D.F.**
1995: Mississippi Valley-Type lead-zinc; *in* Geology of Canadian Mineral Deposit Types, (ed.) O.R. Eckstrand, W.D. Sinclair, and R.I. Thorpe; Geological Survey of Canada, Geology of Canada, no. 8, p. 253–261 (also Geological Society of America, Geology of North America Series P-1).

**Sangster, D.F. and Carrière, J.J.**
1991: Preliminary studies of fluid inclusions in sphalerite from the Robb Lake Mississippi Valley-type deposit, British Columbia; *in* Current Research, Part E, Geological Survey of Canada, Paper 91-1E, p. 25–32.

**Skall, H.**
1975: The paleoenvironment of the Pine Point lead-zinc district; Economic Geology, v. 70, p. 22–47.

**Tesler, H.**
1999: Significance of inclusion fluid chemistry for the origin of the Pine Point mineralization, NWT; M.Sc. thesis, University of Leoben, Leoben, Austria, 99 p.

**Thompson, R.I.**
1989: Stratigraphy, tectonic evolution and structural analysis of the Halfway River map area (94B), northern Rocky Mountains, British Columbia; Geological Survey of Canada, Memoir 425, 119 p.

**Turner, R.J.W., Goodfellow, W.D., and Taylor, B.E.**
1989: Isotopic geochemistry of the Jason stratiform sediment-hosted zinc-lead deposit, MacMillan Pass, Yukon; *in* Current Research, Part E; Geological Survey of Canada, Paper 89-1E, p. 21–30.

**Turner, W.A.**
2006: Microthermometric study of fluids associated with Pb-Zn mineralization in the vicinity of the Pine Point mining camp; *in* Potential for Carbonate-hosted Lead-zinc Mississippi Valley-type Mineralization in Northern Alberta and Southern Northwest Territories: Geoscience Contributions, Targeted Geoscience Initiative, (ed.) P.K. Hannigan; Geological Survey of Canada, Bulletin 591.

**Turner, W.A., Pierce, K.L., and Cairns, K.A.**
2002: Great Slave Reef (GSR) project drillhole database. A compilation of the drillhole locations, drill logs, and associated geochemical data for the Great Slave Reef Joint Venture Project; Interior Platform, Northwest Territories, Canada (85B11 to 14); C.S. Lord Northern Geoscience Centre, NWT Open Report 2002-001, CD-ROM.

**Veizer, J., Ala, D., Azmy, K., Bruckschen, P., Buhl, D., Bruhn, F., Carden, G.A.F., Diener, A., Ebneth, S., Godderis, Y., Jasper, T., Korte, C., Pawellek, F., Podlaha, O.G., and Strauss, H.**
1999: $^{87}Sr/^{86}Sr$, $\delta^{13}C$ and $\delta^{18}O$ evolution of Phanerozoic seawater; Chemical Geology, v. 161, p. 59–88.

**Wedepohl, K.H., Delevaux, M.H., and Doe, B.R.**
1978: The potential source of lead in the Permian Kupferschiefer Bed of Europe and some selected Paleozoic mineral deposis in the Federal Republic of Germany; Contributions to Mineralogy and Petrology, v. 65, no. 3, p. 273–281.

**Wendte, J., Qing, H., Dravis, J.J., Moore, S.L.O., Stasiuk, L.D., and Ward, G.**
1998: High-temperature saline (thermoflux) dolomitization of Devonian Swan Hills platform and bank carbonates, Wild River area, west-central Alberta; Bulletin of Canadian Petroleum Geology, v. 46, no. 2, p. 210–265.

**Yang, W., Spencer, R.J., and Krouse, H.R.**
1995: Stable isotope and major element compositions of fluid inclusions in Devonian and Cambrian dolomite cements, western Canada; Geochimica et Cosmochimica Acta, v. 59, no. 15, p. 3159–3172.